Interfactions between thin- and thick-skinned tectonics at the northwestern front of the Jura fold-and-thrust belt (eastern France)

Herfried Madritsch, Stefan Schmid, Olivier Fabbri

Interactions between thin- and thick-skinned tectonics at the northwestern front of the Jura fold-and-thrust belt (eastern France)

Herfried Madritsch,[1] Stefan M. Schmid,[1] and Olivier Fabbri[2]

Received 26 February 2008; revised 6 June 2008; accepted 18 June 2008; published 4 October 2008.

[1] This study investigates spatial and temporal interactions of thin- and thick-skinned tectonics in a classical foreland setting located at the front of the Jura fold-and-thrust belt in eastern France. The working area coincides with the intracontinental Rhine-Bresse Transfer Zone and represents the most external front of the deformed Alpine foreland. The investigation combines analyses of largely unpublished and newly available subsurface information with our own structural data, including an exhaustive paleostress analysis and geomorphologic observations. Results are provided in the form of a new tectonic map and a series of regional cross sections through the study area. The Besançon Zone, forming the most external part of the thin-skinned fold-and-thrust belt, encroached onto the Eo-Oligocene Rhine-Bresse Transfer Fault System until early Pliocene times. Thrust propagation was largely controlled by the Late Paleozoic to Paleogene preexisting fault pattern that characterizes the Rhine-Bresse Transfer Zone. Thick-skinned deformation, dominant throughout the Avant-Monts Zone located farther to the west, was associated with compressional to transpressional reactivation of such faults. Overprinting and crosscutting criteria of fault slip data allow distinguishing between systematically fanning maximum horizontal stress axes that define the front of the thin-skinned Jura fold-and-thrust belt and consistently NW–SE directed maximum horizontal stress axes that characterize deformation of the autochthonous cover of the foreland, which is affected by thick-skinned tectonics. Tectonic and geomorphic analyses indicate that thick-skinned tectonics started at a very late stage of foreland deformation (post-early Pliocene). Geomorphic observations imply that deformation between Mesozoic cover and basement is locally still decoupled. However, overprinting relationships and recent seismicity suggest that present-day tectonic activity is thick skinned, which probably reflects ongoing tectonic underplating in the Alpine foreland.
Citation: Madritsch, H., S. M. Schmid, and O. Fabbri (2008), Interactions between thin- and thick-skinned tectonics at the northwestern front of the Jura fold-and-thrust belt (eastern France), *Tectonics*, *27*, TC5005, doi:10.1029/2008TC002282.

1. Introduction

[2] During the evolution of an orogenic wedge, transmission of collision-related compressional stresses into the foreland can give rise to thin- or thick-skinned foreland deformation. The tectonic style of foreland deformation is controlled by the level at which decoupling (or décollement) at the base of the orogenic wedge occurs: near the basement-cover interface, within the basement of the upper crust, or even deeper within the lithosphere [*Ziegler et al.*, 2002].

[3] According to the definition of *Chapple* [1978], thin-skinned deformation involves the development of a shallow, gently dipping décollement horizon composed of rheologically weak rocks such as evaporites or shales typically located near or at the base of a sedimentary cover sequence. Rocks immediately beneath the basal décollement level, including the crystalline basement, remain undeformed and become shortened elsewhere, i.e., in the more internal parts of the orogen. The wedge geometry of the deformed sedimentary cover above the décollement and the mechanics of thin-skinned foreland fold-and-thrust belts are described by the critical taper theory [*Chapple*, 1978; *Davis et al.*, 1983].

[4] Conversely, thick-skinned deformation, as used in this contribution, involves deformation within the crystalline basement that underlies the sedimentary sequence; crystalline basement and sedimentary cover are deformed together. Basement shortening in the foreland of the orogen requires the existence of a crustal-scale décollement that allows for the transmission of compressional orogenic stresses [*Coward*, 1983]. The crustal décollement may ramp up into shallow upper crustal levels or extend far out into the foreland, causing inversion of sedimentary basins. In both cases, thick-skinned deformation mostly involves the compressional to transpressional reactivation and inversion of preexisting crustal discontinuities [*Lacombe and Mouthereau*, 2002; *Ziegler et al.*, 2002; *Pfiffner*, 2006].

[5] The concepts of thin- and thick-skinned tectonics represent extreme cases, and transitions between the two modes of contractional deformation may occur (e.g., "base-

[1]Geologisch-Paläontologisches Institut, University of Basel, Basel, Switzerland.
[2]UMR Chrono-Envrionnement, Université de Franche-Comté, Besançon, France.

0278-7407/08/2008TC002282

ment involved thin-skinned tectonics" of *Pfiffner* [2006, p. 153]). The understanding of the way thin- and thick-skinned tectonics interact in space and time represents a key question for the dynamics of foreland deformation in collisional orogens, particularly regarding the sequence of deformation in foreland fold-and-thrust belts. Accordingly, many studies addressed this topic in recent years and revealed complex interferences of the different tectonic styles, also in fold-and-thrust belts that have long been treated as classical examples of thin-skinned deformation, such as the Apennines [*Tozer et al.*, 2002; *Calabrò et al.*, 2003], the Zagros fold-and-thrust belt [*Molinaro et al.*, 2005; *Mouthereau et al.*, 2007] or the fold-and-thrust belt of NW Taiwan [*Lacombe et al.*, 2003]. The sequence of deformation events in foreland settings that are characterized by different deformational styles is very difficult to establish and is variable within different natural settings [*Lacombe and Mouthereau*, 2002]. Thick-skinned deformation often sets in during a late stage of deformation and follows initial thin-skinned tectonics; this potentially leads to thick-skinned refolding of shallow thin-skinned thrust nappes [*Molinaro et al.*, 2005]. On the other hand, there are also natural examples where thick-skinned tectonics occurred during initial stages of foreland deformation far in front of the orogen, controlling the later development of the thin-skinned foreland fold-and-thrust belt [*Lacombe et al.*, 2003].

[6] This study analyzes and discusses temporal and spatial interactions of thin- and thick-skinned tectonics that characterize the northwestern front of the Jura fold-and-thrust belt in eastern France, that is the most external part of the Alpine orogen. Discussions regarding the formation and tectonic style of the Jura fold-and-thrust belt date back to the beginning of the last century (see review by *Sommaruga* [1997]). Although some authors considered pure thick-skinned formation of this fold-and-thrust belt [*Aubert*, 1945; *Pavoni*, 1961], the large majority of authors agree that it initially developed along a shallow décollement horizon formed by Middle to Late Triassic evaporites and that it, hence, represents the type example of a thin-skinned foreland fold-and-thrust belt [*Buxtorf*, 1907; *Laubscher*, 1961; *Burkhard*, 1990; *Burkhard and Sommaruga*, 1998]. However, in addition to thin-skinned deformation, a thick-skinned tectonic style, involving compressional to transpressional reactivation of preexisting basement discontinuities in front, beneath and in the immediate hinterland of the Jura fold-and-thrust belt, was also reported [*Guellec et al.*, 1990; *Pfiffner et al.*, 1997; *Rotstein and Schaming*, 2004; *Ustaszewski and Schmid*, 2007]. Both deformation styles apparently occurred during the latest stages of the evolution at the northwesternmost edge of the Alpine collision zone, i.e., during Neogene to recent times. The exact timing and the mutual relations between these two styles of deformation are, however, ill defined and still controversial.

[7] For the first time, this contribution provides evidence for thick-skinned deformation from the northwestern front of the thin-skinned fold-and-thrust belt. The study focuses on the time constraints regarding the two contrasting styles of deformation by analyzing and discussing subsurface, structural, geomorphic and geophysical data. Thereby it also contributes to the ongoing scientific debate as to which style of deformation and associated stress field characterizes the neotectonic activity along the northwestern front of the Jura Mountains [e.g., *Becker*, 2000]. Ongoing deformation in the area is indicated by low to medium seismicity [*Deichmann et al.*, 2000; *Kastrup et al.*, 2004] and, additionally, by ample evidence for ongoing deformation provided by studies in tectonic geomorphology [*Dreyfuss and Glangeaud*, 1950; *Campy*, 1984; *Giamboni et al.*, 2004; *Madritsch*, 2008]. The question whether thin-skinned, thick-skinned, or a combination of both modes are active at present is of prime importance for any seismic hazard assessment [*Meyer et al.*, 1994; *Nivière and Winter*, 2000; *Ustaszewski and Schmid*, 2007].

2. Tectonic Setting

[8] The area of investigation is part of the northwestern foreland of the European Alps and is located in eastern France (Figure 1). Furthermore, it coincides with the Rhine-Bresse Transfer Zone (RBTZ) [*Laubscher*, 1970; *Illies and Greiner*, 1978; *Bergerat and Chorowicz*, 1981], a central segment of the European Cenozoic Rift System. The latter extends over a distance of approximately 1100 km from the North Sea coast to the western Mediterranean [*Ziegler*, 1992]. The formation of this rift system is interpreted to result from the buildup of syncollisional compressional intraplate stresses in the forelands of the Pyrenees and the Alps [*Dèzes et al.*, 2004]. Late Eocene to Oligocene extension led to the opening of the NNE–SSW striking Rhine and Bresse grabens (Figure 1). The ENE–WSW striking RBTZ cuts trough the autochthonous Mesozoic sediments of the Burgundy Platform and is inferred to have transferred crustal extension between the Rhine and Bresse grabens by sinistral strike-slip motion under ongoing north-south compression [*Bergerat*, 1977] or, alternatively, by sinistral transtension or oblique extension in an roughly E–W oriented extensional stress field [e.g., *Lacombe et al.*, 1993; *Madritsch*, 2008] (inset of Figure 2).

[9] The formation and evolution of the European Cenozoic Rift System, and particularly that of the RBTZ, was clearly controlled by structural inheritance of preexisting Late Paleozoic basement faults that are part of the Burgundy Trough (Figure 2) [*Laubscher*, 1970; *Bergerat and Chorowicz*, 1981; *Schumacher*, 2002; *Madritsch*, 2008]. This ENE–WSW striking Permo-Carboniferous graben system, which parallels the later formed Cenozoic RBTZ (Figure 2), extends from the northern French Massif Central in the west to the southern end of the Rhine Graben in the east, where it connects with the graben systems of northwestern Switzerland and southern Germany [*Boigk and Schönreich*, 1970; *Debrand-Passard and Courbouleix*, 1984; *Ziegler*, 1992; *Diebold and Noack*, 1997]. Its formation is probably related to the activity of a Late Variscan, dextrally transtensive, trans-European shear zone [*Ziegler*, 1986; *Schumacher*, 2002; *McCann et al.*, 2006]. In the western part of the study area, the Burgundy Trough includes the La Serre Horst (LSH in

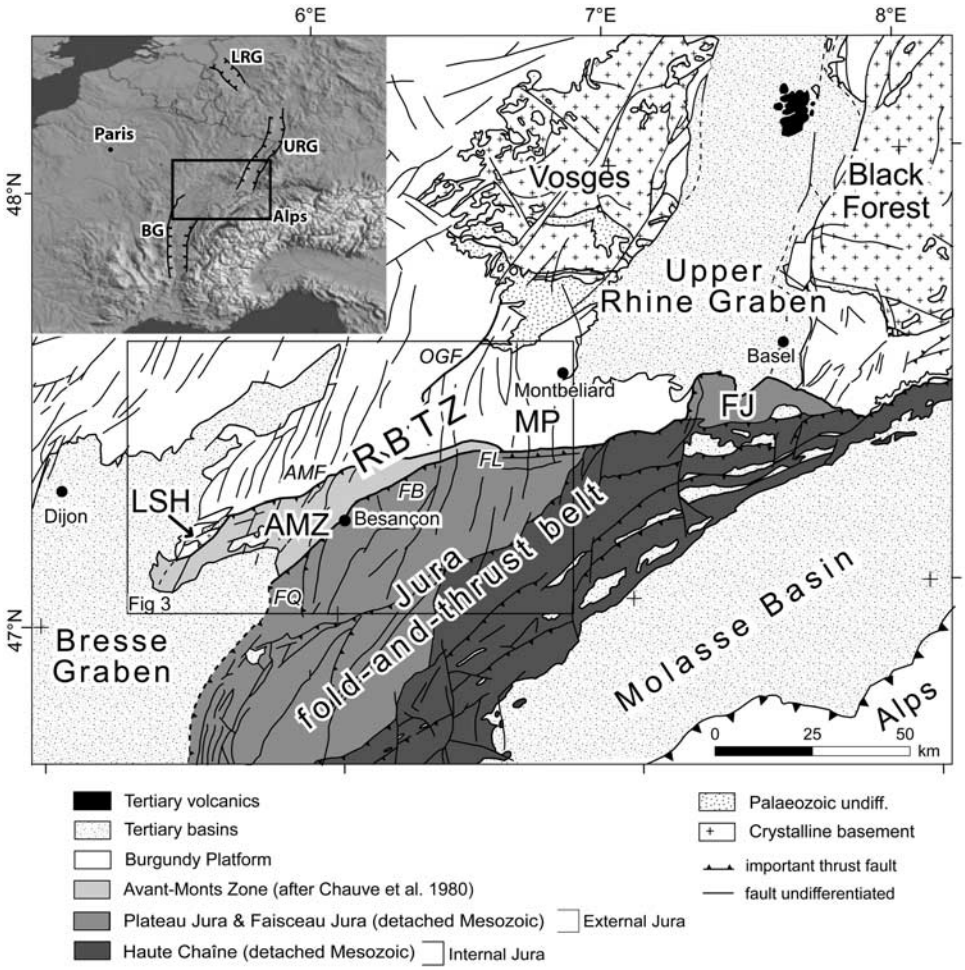

Figure 1. Geological setting of the study area. Subdivisions of the Jura fold-and-thrust belt are taken from *Chauve et al.* [1980]. Note the difference between this classical subdivision and the new subdivision of the Avant-Monts Zone based on the results of this study, as presented in Figure 3. AMF, Avant-Monts Fault; AMZ, Avant-Monts Zone as defined by *Chauve et al.* [1980]; FB, Faisceau Bisontin; FL, Faisceau du Lomont; FQ, Faisceau de Quingey; FJ, Ferrette Jura; LSH, La Serre Horst; MP, Montbéliard Plateau; OGF, Ognon Fault; RBTZ, Rhine-Bresse Transfer Zone. Inset LRG, Lower Rhine Graben; URG, Upper Rhine Graben; BG, Bresse Graben.

Figure 1). This horst exposes pre-Mesozoic strata and is part of a larger Late Paleozoic structural high, the La Serre Horst Structure (LSHS in Figure 2) that extends westward into the Bresse Graben [*Rat*, 1976; *Chauve et al.*, 1983; *Coromina and Fabbri*, 2004; *Madritsch*, 2008]. The reactivation of these Late Paleozoic structures during the Eo-Oligocene formation of the Rhine-Bresse Transfer Zone resulted in a complex pattern of intersecting NNE–SSW and ENE–WSW striking normal faults [*Lacombe et al.*, 1993; *Madritsch*, 2008].

[10] During the early Miocene the crustal stress field in the area of investigation changed. This was due to fundamental changes in deformation processes at the lithosphere scale and related to ongoing Alpine collision [*Bergerat*, 1987; *Dèzes et al.*, 2004]. The Jura fold-and-thrust belt whose northwestern rim parallels the RBTZ (Figure 1) formed in response to this stress field change. The some 400 km long belt is bounded to the SE by the rigidly displaced flexural Molasse Basin and hence represents the northwestern deformation front of the Alpine orogen.

[11] The Jura fold-and-thrust belt is considered as a type example for a thin-skinned foreland fold-and-thrust belt and its initial formation is nowadays widely accepted to be the result of distant push (''Fernschub'') [*Buxtorf*, 1907; *Laubscher*, 1961, 1978; *Burkhard*, 1990; *Sommaruga*, 1997; *Sommaruga and Burkhard*, 1997]. Crustal shortening and nappe stacking in the external crystalline massifs of the Alps induced a decoupling of deformation between the undeformed crystalline basement that gently dips toward the hinterland and the detached Mesozoic cover along Middle to Late Triassic evaporites [*Burkhard*, 1990; *Schmid et al.*, 1996; *Burkhard and Sommaruga*, 1998]. The Mesozoic cover was displaced far into the northern foreland. Horizontal shortening estimates from balanced cross sec-

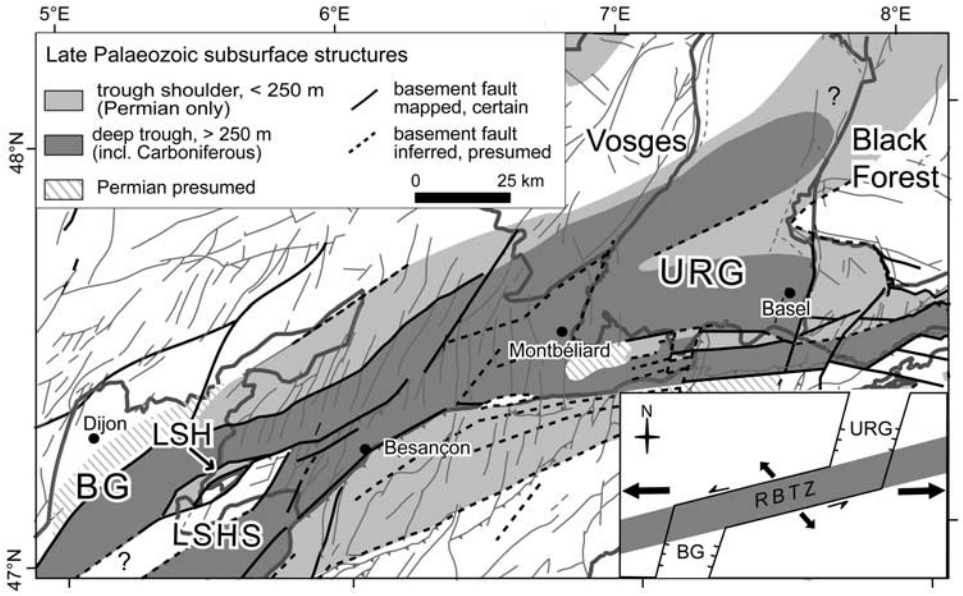

Figure 2. Subsurface map of the Rhine-Bresse Transfer Zone (RBTZ) showing the Late Paleozoic Burgundy Trough (modified after *Debrand-Passard and Courbouleix* [1984], and *Ustaszewski et al.* [2005b]). BTS, Burgundy Trough system; LSH, La Serre Horst; RBTZ, Rhine-Bresse Transfer Zone. Inset shows the conceptual model for the Eo-Oligocene formation of the RBTZ proposing sinistral transtensive reactivation of this preexisting Paleozoic fault system (modified from *Lacombe et al.* [1993]). BG, Bresse Graben; LSHS La Serre Horst Structure; URG, Upper Rhine Graben.

tions across the arcuate shaped fold-and-thrust belt range from zero at its northeastern termination to an average of about 30 km in its central part [*Burkhard*, 1990; *Philippe et al.*, 1996]. At its northern and western rim the Jura fold-and-thrust belt encroached onto the European Cenozoic Rift System [*Laubscher*, 1986; *Guellec et al.*, 1990; *Ustaszewski and Schmid*, 2006]. Preexisting extensional structures related to the rift system did not only control the geometry and distribution of the most frontal thin-skinned thrusts and folds but also the propagation style of the entire fold-and-thrust belt that typically features divergent stress and strain trajectories toward the deformation front [*Laubscher*, 1972; *Philippe et al.*, 1996; *Hindle and Burkhard*, 1999; *Homberg et al.*, 1999; *Affolter and Gratier*, 2004].

[12] Most authors consider the formation of the thin-skinned Jura fold-and-thrust belt as a rather short-lived event. Near its northern rim a maximum age for the onset of thin-skinned deformation is inferred from the Bois de Raube formation, which reveals a biostratigraphic age between 13.8 and 10.5 Ma years and whose sedimentation predates thin-skinned Jura folding in that area [*Kälin*, 1997]. A maximum age of 9 Ma can be inferred from the western front of the Jura where this fold-and-thrust belt thrusted the Bresse Graben [*Guellec et al.*, 1990; *Becker*, 2000].

[13] Termination of thin-skinned Jura folding is less well constrained. Undeformed karst sediments have been detected in a fold limb located in the central part of the fold-and-thrust belt; their biostratigraphic age implies that folding terminated before some 4.2–3.2 Ma ago in this area [*Bolliger et al.*, 1993; *Steininger et al.*, 1996]. In the case that propagation of the fold-and-thrust belt toward the foreland was in sequence, which is not always the case as illustrated by the results of recent analog models [*Costa and Vendeville*, 2002; *Smit et al.*, 2003], thin-skinned deformation may have operated longer in the more external parts of the fold-and-thrust belt [*Ustaszewski and Schmid*, 2006]. Evidence for ongoing deformation from the northern and northwestern front of the fold-and-thrust-belt is indeed provided by studies in tectonic geomorphology [*Dreyfuss and Glangeaud*, 1950; *Campy*, 1984; *Meyer et al.*, 1994; *Nivière and Winter*, 2000; *Giamboni et al.*, 2004; *Madritsch*, 2008].

[14] The style of post-early Pliocene and recent deformation, however, is a matter of debate. While some authors proposed that thin-skinned deformation is presently still ongoing [*Nivière and Winter*, 2000; *Müller et al.*, 2002], others, on the basis of the interpretation of seismic reflection data, proposed that thick-skinned present-day activity affects the frontal-most Jura folds [*Giamboni et al.*, 2004; *Rotstein and Schaming*, 2004; *Ustaszewski and Schmid*, 2006]. *Giamboni et al.* [2004] and *Ustaszewski and Schmid* [2007] hold this type of deformation exclusively responsible for all post-2.9 Ma folding of the middle-late Pliocene Sundgau gravels. According to these authors, ongoing thick-skinned deformation involves the inversion of Paleozoic and/or Paleogene basement faults in dextral transpression. On the basis of their observations, made east of our area of investigation and at the southern rim of the Rhine Graben (Figure 1), they proposed that thick-skinned deformation postdated thin-skinned Jura folding and that thin-skinned thrusting came to a halt by the early Pliocene. However, this remains a hypothesis, and furthermore, it is a

matter of debate as to whether this proposition applies for the area of the Rhine-Bresse Transfer Zone, i.e., over the entire length of the front of the Jura fold-and-thrust belt. Moreover, a temporal coexistence of both styles of deformation, before or after the early Pliocene, cannot be excluded [*Meyer et al.*, 1994; *Nivière and Winter*, 2000]. This study will add new field and subsurface data in order to test such hypotheses over a large area located along the northwestern front of the Jura fold-and-thrust belt (Figure 1).

[15] Commonly the Jura fold-and-thrust belt is divided into two major parts [*Chauve et al.*, 1980; *Philippe et al.*, 1996; *Sommaruga*, 1997] (Figure 1): (1) The internal or ''folded'' Jura, which features intense shortening along the discrete southeastern border adjacent to the Molasse basin and which is characterized by major folds, thrusts and tear faults, and (2) the more external Plateau Jura farther to the north, which comprises largely undeformed tabular areas (''plateaus''), separated by narrow zones of intense deformation. The latter form discrete map-scale linear structures (''faisceaux'') along which shortening is concentrated. The ENE–WSW striking Faisceau Bisontin is the northwesternmost of these narrow deformation zones. Eastward it connects with the Faisceau du Lomont; southwestward it splays into north-south striking deformation zones, the Faisceau de Quingey being the most prominent and external one (Figure 1). The latter clearly marks the western border of the Jura fold-and-thrust belt with the Eo-Oligocene Bresse Graben.

[16] The exact location of the northwestern front of the thin-skinned Jura fold-and-thrust belt is still ill defined. A large area northwest of the Faisceau Bisontin, often referred to as Avant-Monts Zone, is also weakly deformed (Figure 1) [*Chauve et al.*, 1980; *Philippe et al.*, 1996; *Sommaruga*, 1997], but it remains unclear whether this area is also part of the thin-skinned taper. The prominent ENE–WSW striking Avant-Monts Fault and the westerly adjacent La Serre Horst define the northern boundary of the Avant-Monts Zone (AMZ in Figure 1) toward the Burgundy Platform that shows no signs of contractional deformation (Figure 1). Another zone of weak shortening, the Montbéliard Plateau (MP in Figure 1), is located farther east and also north of the supposed front of the thin-skinned fold-and-thrust belt (Faisceau du Lomont, FL in Figure 1). Gentle folding is observed well north of the Faisceau du Lomont all the way toward the southwestern rim of the Rhine Graben [*Giamboni et al.*, 2004]; the easternmost folds north of the Faisceau de Lomont and within our study area terminate near the city of Montbéliard [*Contini et al.*, 1973]. However, previous authors did not consider this area as part of the Avant-Monts Zone nor as belonging to the thin-skinned Jura fold-and-thrust belt [*Chauve et al.*, 1980; *Philippe et al.*, 1996; *Sommaruga*, 1997]. It remains unclear whether all the above mentioned weakly deformed areas were also a part of the thin-skinned fold-and-thrust belt or whether they were deformed in a thick-skinned manner. The locations of the Avant-Monts Zone and the Montbéliard Plateau coincide with the RBTZ that was reported to have been reactivated in a transpressional, thick-skinned manner east to our study area [*Giamboni et al.*, 2004]. Hence, in regard to expected interactions between thin and thick-skinned styles of deformation, the Avant-Monts Zone and similar weakly deformed areas at the front of the Jura fold-and-thrust belt are of special interest to this study.

[17] For clarity, we had to propose a new tectonic subdivision, presented in Figure 3 and discussed in sections 3.1 and 3.2, when presenting our data. We subdivide the areas located north of the well defined and substantially detached parts of the thin-skinned Jura fold-and-thrust belt, i.e., the areas which feature weak contractional deformation, as follows, going from west to east: (1) the Avant-Monts Zone that will turn out to be dominated by thick-skinned deformation, (2) the Besançon Zone for which we will present evidence for a thin-skinned style of deformation, bordered by the Chailluz Thrust to the north, and (3) the Montbéliard Plateau in the east, only mildly affected by Neogene deformation and largely characterized by thick-skinned deformation.

3. Results

3.1. Subsurface Analysis

[18] The locations of the subsurface data analyzed are given in Figure 4. Geological logs of boreholes, dating back to the early 20th century, were obtained from the BRGM archive. These reports also include results of reflection seismic campaigns carried out by Safrep in the 1950s yielding additional subsurface information. Total and Gaz de France generously provided more recent seismic reflection data, those of Gaz de France being accessible to an academic institution for the first time. All of the seismic reflection data have been commercially processed and were available to us for interpretation in form of a paper copy.

[19] The analyses and correlations of borehole and seismic reflection data revealed significant differences in the structural style that occur at the northern rim of the Avant-Monts Zone and the Besançon Zone, i.e., along the strike of the prominent ENE–WSW Avant-Monts Fault (''AMF'' in Figure 1).

[20] A borehole located at Chailluz (Figures 4, 5, and 6) in the Besançon Zone, and immediately south of the Avant-Monts Fault, provides key information. It reveals a low-angle thrust fault at a depth of 113 m (Figure 6). In the subsurface this thrust places Triassic evaporites over Late Jurassic limestones. The associated anticline was mapped as the ''Chailluz Anticline'' at the surface and is interpreted as a thrust related fault bend fold [*Suppe*, 1983]. Undoubtedly, this structure is typical for the thin-skinned style of the Jura fold-and-thrust belt [*Martin and Mercier*, 1996], that is well documented and described by seismic reflection data throughout the more internal parts of the Jura fold-and-thrust belt [*Sommaruga*, 1997]. Hence, we regard the Besançon Zone as a part of the northwestern most thin-skinned Jura fold-and-thrust belt, which propagated into an area located well north of the Faisceau Bisontin (Figure 5). The segment of the Avant-Monts Fault bordering the Besançon Zone to the north is defined as the Chailluz Thrust and represents the outer most thrust of the thin-skinned Jura. This is the principal reason for separating the

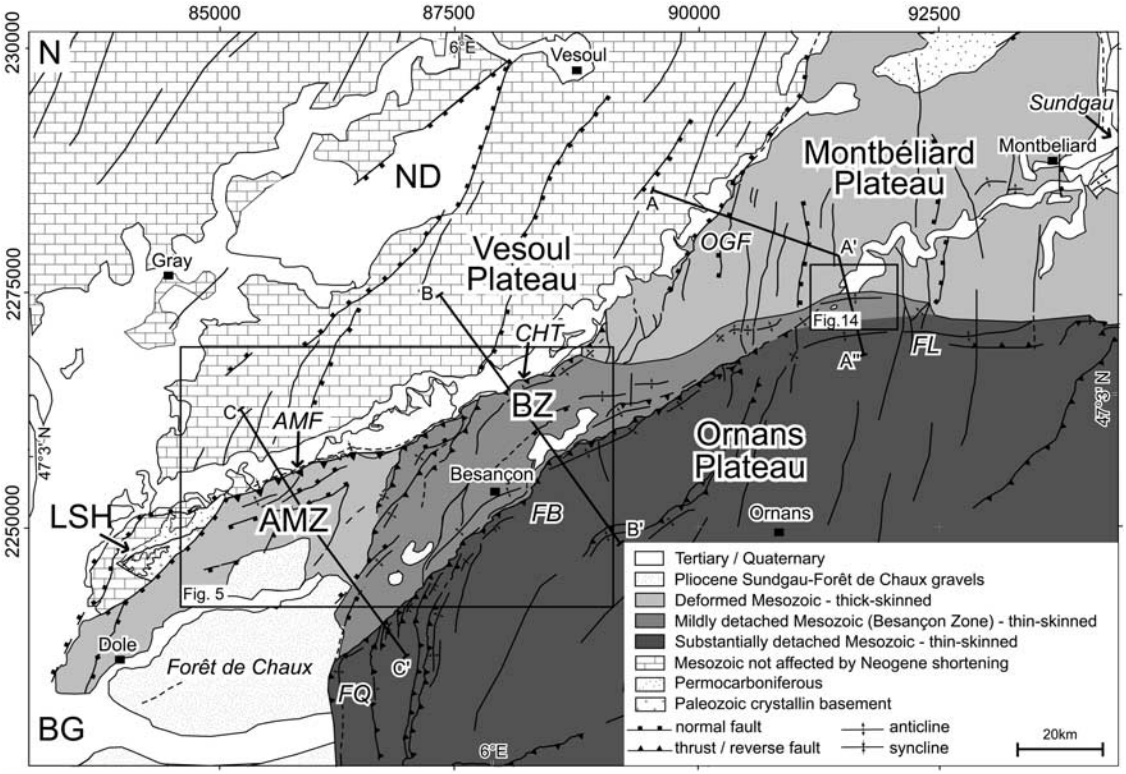

Figure 3. Tectonic map of the study area, showing the new subdivision based on the results of this study (see text for discussion). Note the traces of three cross sections shown in Figure 8. AMF, Avant-Monts Fault; AMZ, Avant-Monts Zone; BZ, Besançon Zone; BG, Bresse Graben; CHT, Chailluz Thrust; FB, Faisceau Bisontin; FL, Faisceau du Lomont; FQ, Faisceau de Quingey; LSH, La Serre Horst; ND, Noidans Basin; OGF, Ognon Fault.

Besançon Zone from the Avant-Monts Zone located farther to the west (Figure 3) where we found no indications for such shallow decoupling, as discussed below.

[21] Farther west, along strike of the Avant-Monts Fault, the Moutherot borehole penetrated another anticline (the Moutherot Anticline; Figures 5 and 6). This borehole, however, displays an undisturbed Mesozoic succession. The potential décollement in Middle to Late Triassic evaporites was not tectonically thickened (Figure 6) and remained undeformed. Hence, the previously described low-angle Chailluz Thrust detected in borehole Chailluz cannot be traced along strike farther to the west. This indicates that the front of the decoupled Jura fold-and-thrust belt steps back from the Avant-Monts Fault along a series of NNE–SSW striking transverse structures, which delimit the Besançon Zone from the Avant-Monts Zone located farther west. Ultimately these transverse structures link up with the Faisceau de Quingey (see Figure 3).

[22] Furthermore, newly available seismic reflection data across the Avant-Monts Zone provided by Gaz de France (Figure 7) lack evidence for a thin-skinned origin of the Moutherot Anticline. The logs from the Moutherot and Gendrey 1 wells (Figure 6) allowed for the calibration of the reflectors of this seismic section. Both boreholes are located in the immediate vicinity of the seismic line

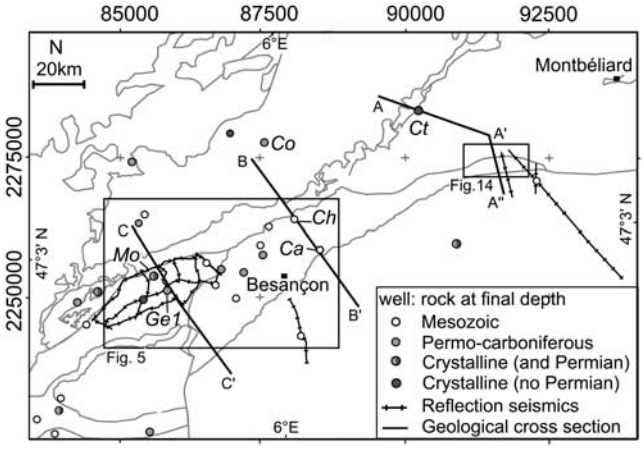

Figure 4. Map depicting the location of subsurface data analyzed in this study and traces of regional cross sections shown in Figure 8. Wells used for the construction of the regional cross sections depicted in Figure 8 are labeled in italics. Gray lines indicate the outlines of the tectonic units shown in Figure 3.

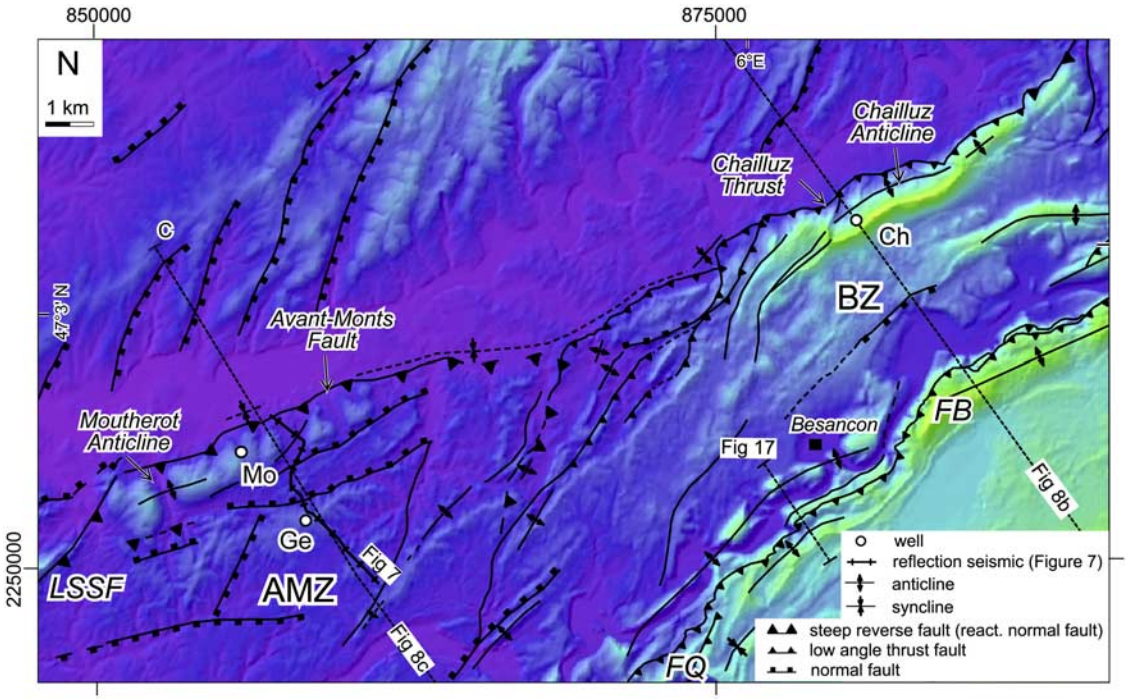

Figure 5. Shaded digital elevation model (horizontal resolution 50 m) and structural map of the central part of the Rhine-Bresse Transfer Zone. The anticlines near the Moutherot and Chailluz wells are both aligned along the ENE–WSW striking Avant-Monts Fault. The boundary between the Besançon Zone and the Avant-Monts Zone, as mapped in Figure 3, is marked by an array of minor folds and thrust faults striking NNE–SSW, located in the center of this figure and west of the city of Besançon. The locations of wells shown in Figure 6, the trace of the seismic reflection line shown in Figure 7 and those of the geological profiles of Figures 8 and 17 are also given. AMZ, Avant-Monts Zone; BZ, Besançon Zone; FB, Faisceau Bisontin; FQ, Faisceau de Quingey; LSSF, La Serre Southern Fault; Mo, Moutherot well; Ch, Chailluz well; Ge, Gendrey 1 well.

(Figures 4 and 5) and both penetrate the entire Mesozoic succession. The Mesozoic cover sediments are characterized by high-amplitude, continuous reflections. By contrast, the underlying Permian strata recorded in both boreholes feature discontinuous reflections and an occasionally rather chaotic seismic character. In the central part of the seismic section, Permian reflections unconformably top lap against the subhorizontal and continuous Mesozoic reflections; they mark the base Mesozoic angular unconformity.

[23] The top of the Early Triassic Buntsandstein Formation, located at 300 to 350 ms twoi-way traveltime (TWT), provides a well-pronounced reflector that is located below the Middle to Late Triassic evaporites, i.e., the potential décollement horizon. The top of this evaporitic succession, which partly features highly transparent reflections, is again marked by a prominent reflector (50 to 150 ms TWT) that marks the boundary between the top of the Late Triassic Keuper formation and the overlying Liassic marls. This more or less flat-lying sedimentary sequence largely remained undeformed in the southern part of the section. The central part of the seismic section located south of the Avant-Monts Fault, however, displays several E–W striking and steeply north dipping normal faults. These formed during Paleogene extension in the Rhine-Bresse Transfer Zone and they systematically downfault the northern compartments. Most importantly, the westernmost segment of the Avant-Monts Fault, displayed in the northern part of the reflection seismic profile (Figure 7), is clearly seen to represent a steep reverse fault dissecting the entire Mesozoic succession. Hence, this western segment of the Avant-Monts Fault is rooted in the basement and probably represents an inverted former Paleogene normal fault. A contour map of the base Mesozoic in the western Avant-Monts Zone and the area of the La Serre Horst, established on the basis of the entire seismic data set [*Madritsch*, 2008], further supports such an interpretation. Interestingly, normal fault inversion occurs only along the south dipping normal faults whereas the north dipping normal faults appear hardly affected by reactivation. Similar observations are reported from other thick-skinned inversion settings, e.g., the fold-and-thrust belt of northwestern Taiwan [*Lacombe et al.*, 2003].

[24] Farther west, thick-skinned thrusting along the Avant-Monts Fault is kinematically linked to the La Serre Southern Fault [*Coromina and Fabbri*, 2004; *Madritsch*, 2008] which forms the southern boundary of the Late Paleozoic La Serre Horst and which has been reactivated during Paleogene extension and the formation of the Rhine-

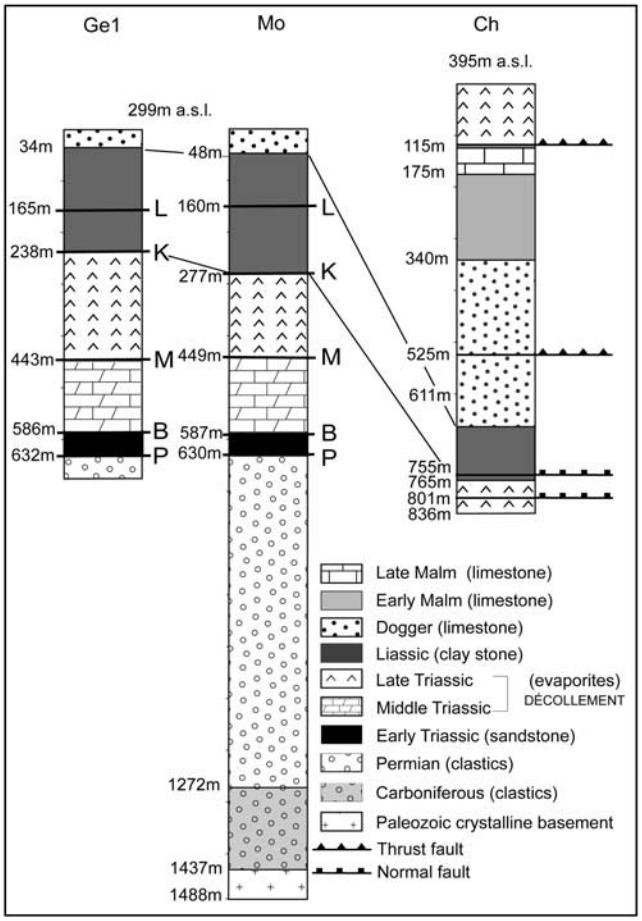

Figure 6. Lithological logs of three deep wells from the Avant-Monts and Besançon zones (see Figures 4 and 5 for locations). Borehole Moutherot (Mo) penetrates the Moutherot Anticline in the Avant-Monts Zone. It displays a continuous sedimentary succession with no indication of low-angle thrust faulting. The correlation with the neighboring Gendrey1 (Ge1) borehole yields no evidence for tectonic thickening of the potential décollement horizon within Middle to Late Triassic evaporites. The borehole Chailluz (Ch) penetrates the Chailluz Anticline located in the frontal part of the Besançon Zone. The low-angle thrust fault at a depth of 115 m emplaces Triassic evaporites over Upper Jurassic limestones, indicating that the Chailluz Anticline is a fault-related fold, typical for thin-skinned deformation. Note that the correlation of the top Liassic horizon between the wells indicates that the Avant-Monts Zone forms a structural high with respect to the Besançon Zone east of it. Also note the stratigraphic position of seismic reflectors L, K, M, and B given in Figure 7.

Bresse Transfer Zone [*Madritsch*, 2008]. This confirms the interpretation that the Avant-Monts Fault, as seen in Figure 7, formed by the inversion of a preexisting Paleogene normal fault, that in turn is inferred to have formed along Late Paleozoic structures (see interpretation in the section of Figure 8c). Note that the small amplitude of the Moutherot Anticline (Figures 6, 7, and 8c), formed as a result of thick-skinned normal fault reactivation, only features a very gentle surface expression (Figure 5) and is hardly visible in the seismic reflection image (Figure 7). This implies that the amount of shortening of the Mesozoic cover associated with this structure is smaller than that associated with thin-skinned fault-related folding above the low-angle Chailluz Thrust farther to the east.

[25] In summary, thick-skinned shortening observed throughout the Avant-Monts Zone strongly contrasts with the thin-skinned style of deformation found in the Besançon Zone, where the frontal Chailluz Thrust is soling off as a low-angle listric thrust fault within the décollement layer provided by the Late Triassic evaporites (Figure 8b).

3.2. Regional Tectonic Synthesis

[26] The results of the subsurface data analysis (Figures 4, 5, 6, and 7), together with the study of the available geological maps [*Dreyfuss and Kuntz*, 1969, 1970; *Dreyfuss and Théobald*, 1972; *Contini et al.* 1973; *Bonte*, 1975; *Chauve et al.*, 1983], lead to a new tectonic interpretation, and accordingly, the subdivision of units along the northwestern front of the Jura fold-and-thrust belt proposed in Figure 3. The following five different tectonic zones are distinguished:

[27] 1. The Vesoul Plateau is part of the autochthonous European foreland, which lacks map-scale contractional deformation features related to Neogene compression. To the west, the Vesoul Plateau borders the Eo-Oligocene Bresse Graben. Its southern and southeastern border follows the Ognon Fault [*Ruhland*, 1959], a Paleogene age NE–SW striking normal fault that formed along a preexisting Paleozoic discontinuity (see profile A-A′ in Figure 8).

[28] 2. The Avant-Monts Zone features post-Paleogene thick-skinned reactivation of preexisting Paleogene to Paleozoic normal faults and is bordered by the crystalline La Serre Horst in the northwest. It is thus not part of the thin-skinned Jura fold-and-thrust belt.

[29] 3. The newly defined Besançon Zone (formerly considered as the eastern part of the Avant-Monts Zone) is affected by thin-skinned Neogene shortening and hence represents the northwesternmost segment of the Jura fold-and-thrust belt.

[30] 4. The Montbéliard Plateau farther to the east consists of autochthonous Mesozoic strata tilted southward during Miocene age uplift of the Vosges Mountains [*Ziegler*, 1992; *Bourgeois et al.*, 2007]. To the west, the Montbéliard Plateau wedges out between the Ognon Normal Fault in the north and the Besançon Zone in the south. To the east it borders the Rhine Graben. In contrast to the Vesoul Plateau, this area includes isolated anticlines such as those near Montbéliard (Figure 3) [*Contini et al.*, 1973] and was, hence, presumably affected by late Miocene to recent contraction. The origin of these structures, thick- or thin-skinned, remains controversial [*Nivière and Winter*, 2000; *Ustaszewski and Schmid*, 2007].

[31] 5. The Ornans Plateau is part of the Plateau Jura proper and delimited to the northwest by the Lomont, Bisontin, and Quingey deformation zones (faisceaux). While

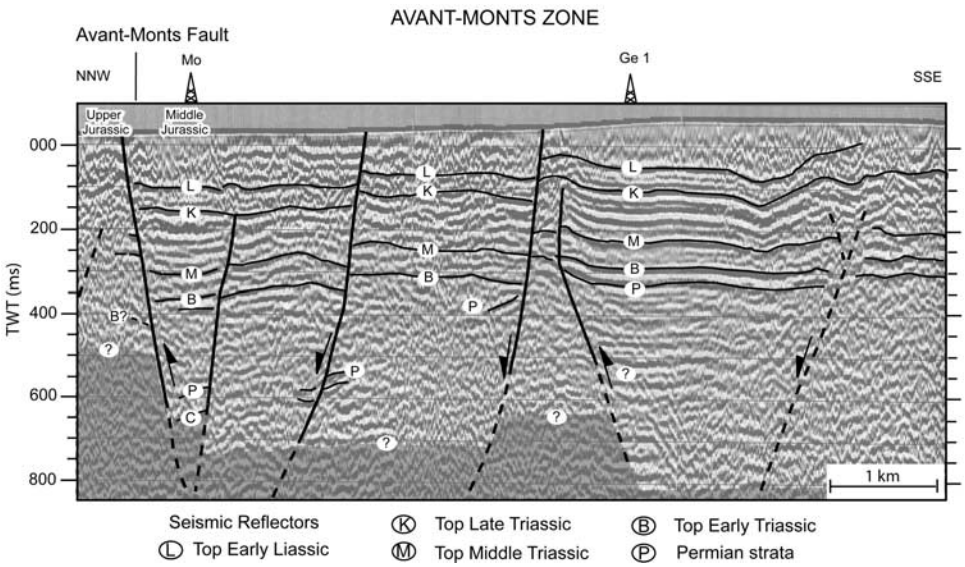

Figure 7. NNW–SSE oriented seismic reflection line across the Avant-Monts Zone (see Figures 4 and 5 for location). Correlations between seismic reflectors and stratigraphy are based on geological logs of boreholes Moutherot and Gendrey 1 (Figure 6). Note that the Avant-Monts Fault in the northern part of the section appears as a steep reverse fault that crosscuts the whole Mesozoic succession, including the supposed décollement horizon within Middle to Late Triassic evaporites (reflector M). This clearly indicates thick-skinned tectonics along this segment of the fault, probably associated with inversion of a preexisting normal fault. (Seismic data courtesy of GAZ de France).

the N–S striking Faisceau de Quingey clearly represents the front of the Jura fold-and-thrust belt toward the Eo-Oligocene Bresse Graben [*Guellec et al.*, 1990], the ENE–WSW striking Faisceau Bisontin is an internal thrust bundle that marks the boundary between Ornans Plateau and Besançon Zone, both these zones being affected by thin-skinned décollement. eastward, the Faisceau Bisontin merges into the E–W striking Faisceau du Lomont, connected with the Mont Terri–Landsberg Line [*Guerler et al.*, 1987].

[32] The sections shown in Figure 8 were constructed by integrating existing geological maps [*Dreyfuss and Kuntz*, 1969, 1970; *Dreyfuss and Théobald*, 1972; *Contini et al.*, 1973; *Bonte*, 1975; *Chauve et al.*, 1983] and our own field measurements with unpublished well data and seismic sections. Well logs yield rather constant thickness of Mesozoic strata that could be extrapolated throughout the area. While several wells document the existence of the Late Paleozoic Burgundy Trough underneath the Mesozoic cover, the overall geometry and location of border faults of this through system are not precisely known [*Debrand-Passard and Courbouleix*, 1984] (Figure 2). We assumed that border faults of the Late Paleozoic trough system predetermined the location of major Paleogene normal faults, generally assumed to have formed by their reactivation [*Laubscher*, 1970; *Illies*, 1972; *Bergerat and Chorowicz*, 1981].

[33] The easternmost section (Figure 8a) crosses the Faisceau du Lomont where the locus of the outermost thin-skinned folds (Clerval Anticline and Lomont Anticline in Figure 8a) appears to be controlled by preexisting normal faults that formed at the southern margin of the Eo-Oligocene Rhine-Bresse Transfer Zone. The latter caused an offset of the Triassic décollement horizon and flexuring of the overlying sediments, structures also described farther east and throughout the southern Upper Rhine Graben area [*Ustaszewski et al.*, 2005a; *Ford et al.*, 2007] as well as throughout the easternmost Jura [*Laubscher*, 1986]. These flexures triggered the formation of thrust-related anticlines during thin-skinned Neogene contraction [*Martin and Mercier*, 1996].

[34] Farther west (Figure 8b), however, the thin-skinned fold-and-thrust belt propagated farther into the foreland, far beyond the Faisceau Bisontin, i.e., in front of the Besançon Zone that encroached far outward, all the way to the Chailluz Anticline and onto the preexisting normal faults of the Rhine-Bresse Transfer Zone. The Chailluz Anticline is associated with the outermost thin-skinned Chailluz Thrust, as is well documented by the Chailluz borehole (Figures 5 and 6) [*Martin and Mercier*, 1996].

[35] The westernmost section (Figure 8c) crosses the Avant-Monts Zone and also integrates a seismic reflection section across the Moutherot Anticline and the western segment of the Avant-Monts Fault (Figures 5, 6, and 7). The latter represents a steep reverse fault that dissects the whole Mesozoic succession and particularly the supposed thin-skinned detachment horizon in Middle to Late Triassic evaporites. It is hence clearly related to basement rooted shortening by thick-skinned inversion of preexisting normal faults; it is not part of classical thin-skinned deformation. In section 8c the front of the Jura fold-and-thrust belt is located farther to the south and once more sketched out by a preexisting Paleogene normal fault. The Routelle Anticline is interpreted to have formed along the normal fault flexure.

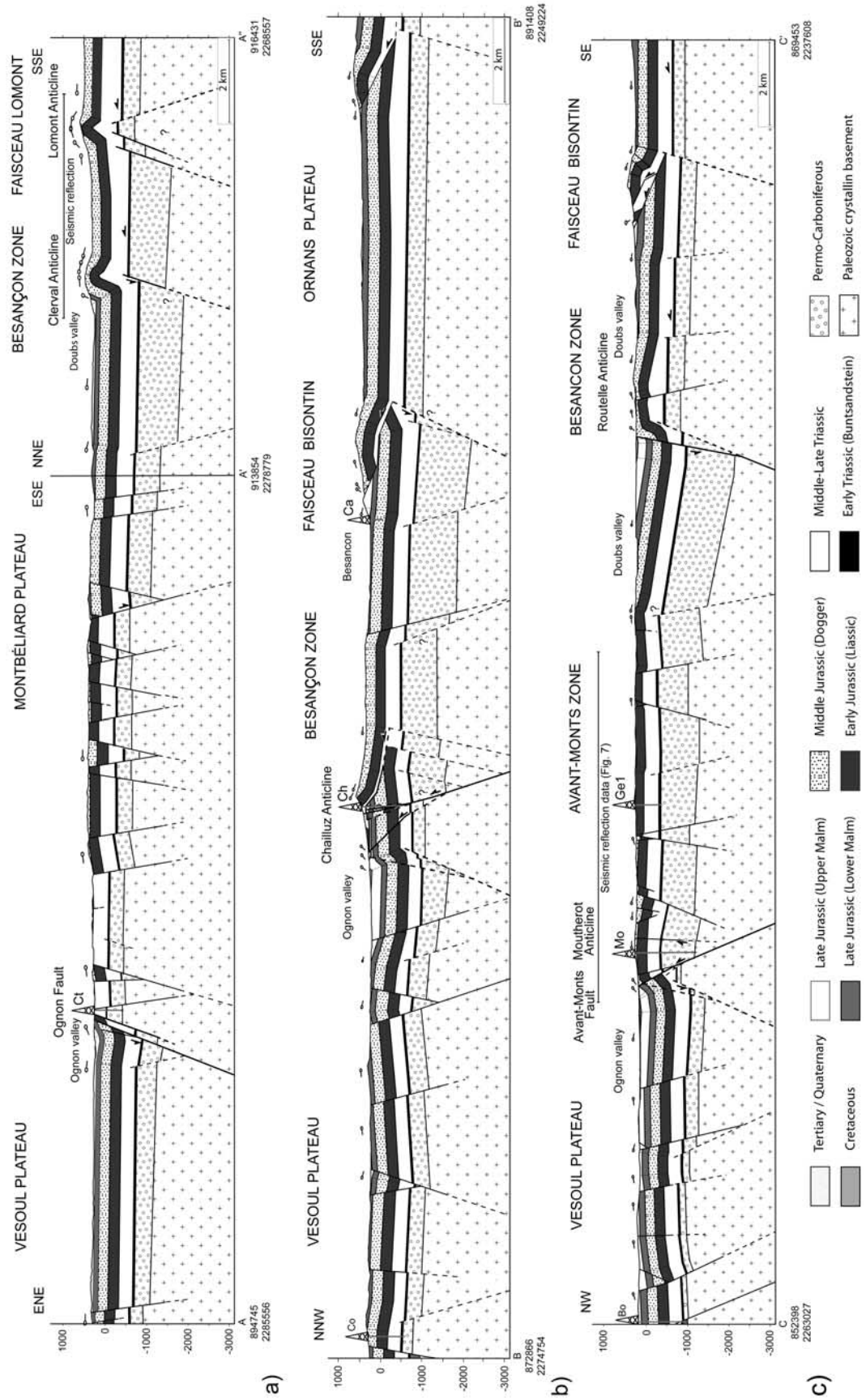
a)
ENE
VESOUL PLATEAU
MONTBÉLIARD PLATEAU
ESE NNE
BESANÇON ZONE
FAISCEAU LOMONT
SSE
Ognon Fault
Ognon valley
Ct
Doubs valley
Clerval Anticline
Seismic reflection
Lomont Anticline
2 km
A
894745
2285556
A'
913854
2278779
A"
916431
2268557
b)
NNW
VESOUL PLATEAU
BESANÇON ZONE
FAISCEAU BISONTIN
ORNANS PLATEAU
SSE
Co
Ognon valley
Chailluz Anticline
Ch
Besancon
Ca
2 km
B
872866
2274754
B'
891408
2249224
c)
NW
VESOUL PLATEAU
AVANT-MONTS ZONE
BESANCON ZONE
FAISCEAU BISONTIN
SE
Bo
Ognon valley
Avant-Monts Fault
Moutherot Anticline
Seismic reflection data (Fig. 7)
Mo
Ge1
Routelle Anticline
Doubs valley
2 km
C
852398
2263027
C'
869453
2237608
Tertiary / Quaternary
Cretaceous
Late Jurassic (Upper Malm)
Late Jurassic (Lower Malm)
Middle Jurassic (Dogger)
Early Jurassic (Liassic)
Middle-Late Triassic
Early Triassic (Buntsandstein)
Permo-Carboniferous
Paleozoic crystallin basement

Figure 8

It is located north to the Faisceau de Quingey and is therefore part of the Besançon Zone.

3.3. Brittle Tectonics and Paleostress Analysis

[36] An extensive analysis of outcrop-scale brittle structures was carried out throughout the study area. This analysis attempted to better constrain possible differences in the kinematics and timing of deformation between areas affected either by a thick- or a thin-skinned or, alternatively, by both styles of deformation.

3.3.1. Methodology

[37] The analysis of fault slip data is based on inferring either incremental strain or stress from a set of fault planes and associated directions of slip. Therefore two different basic hypotheses underlying paleostress methodology can be distinguished.

[38] The kinematic approach assumes that the slip direction on a fault plane is parallel to the maximum resolved shear strain rate governed by a large-scale homogeneous strain rate tensor [*Twiss and Unruh*, 1998]. This approach is considered to be very robust and basically describes the observed displacements. In fact, the results of kinematic "paleostress" analyses yield the approximate orientation of the principal axis of incremental strain based on the graphical or numerical construction of "kinematic axes", or p-t axes, for each fault-slip pair [*Marrett and Allmendinger*, 1990; *Twiss and Unruh*, 1998]. By contrast, the stress hypothesis, also referred to as dynamic analysis, assumes that the slip direction on a fault plane is parallel to the direction of maximum resolved shear stress induced by a large-scale homogenous stress field [*Wallace*, 1951; *Angelier*, 1990]. The results of dynamic analyses yield the orientation of the principal axes of stress ($\sigma1 > \sigma2 > \sigma3$) and in this sense represent a genetic interpretation of the observed structures [*Marrett and Peacock*, 1999].

[39] Besides these principle assumptions, paleostress analysis further assumes that the analyzed rock is physically and mechanical isotropic and behaves as a rheologically linear material [*Twiss and Unruh*, 1998]. Therefore fault orientation in prefractured rocks should be random and different faults should not kinematically interact with each other. *Pollard et al.* [1993] pointed out that these requirements are often unrealistic. However, in cases where displacements on fault planes are small with respect to fault length, these conditions are likely to be fulfilled [*Lacombe et al.*, 2006].

[40] In this study we applied a combined kinematic-dynamic approach by applying the kinematic p-t axes method [*Marrett and Allmendinger*, 1990] as well as the dynamic Right-Dihedra method [*Angelier and Mechler*, 1977; *Pfiffner and Burkhard*, 1987]. The latter method is considered as the simplest but also the most robust dynamic paleostress approach [*Angelier*, 1989]. While Direct Inversion methods calculate a theoretical "best fit" stress tensor and the stress ratio [*Angelier*, 1990], the Right-Dihedra method delivers an estimation of the possible orientations of the principal stress axes with the most likely orientation computed at point maxima of superimposed compressional and tensional dihedra, calculated for each fault slip pair [*Angelier and Mechler*, 1977; *Pfiffner and Burkhard*, 1987]. Therefore the Right-Dihedra method also considers movements along a nonrandom set of preexisting and hence reactivated fault planes that are not necessarily oriented ideally in terms of a theoretical best fit reduced stress tensor. Comparative studies [*Meschede and Decker*, 1993] have shown that the Right-Dihedra method, in contrast to Direct Inversion methods, is less sensitive to highly asymmetric fault plane associations such as commonly found in tectonic settings of polyphase brittle deformation as the study area.

[41] In the northwestern Alpine foreland four consecutive major paleostress fields were proposed to have been active in Cenozoic times [*Bergerat*, 1987]. These were reconstructed by numerous investigations in neighboring areas [*Lacombe et al.*, 1993; *Homberg et al.*, 2002; *Rocher et al.*, 2003] and were also encountered in the course of this study [*Madritsch*, 2008]. These stress fields are (1) NNE–SSW shortening, attributed an early Eocene age by most authors, related to the Pyrenean orogeny, (2) E–W to NW–SE directed extension, related to the Eo-Oligocene formation of the European Cenozoic Rift System, including the Rhine-

Figure 8. Interpretive cross sections based on published maps, structural field measurements and subsurface data (see Figures 3 and 4 for location of sections). (a) Going from SSE to NNW, section AA′A″ first crosses the Faisceau du Lomont which represents the front of the Plateau Jura, the Clerval Anticline farther to north, interpreted as the easternmost part of the Besançon Zone, still affected by thin-skinned Jura folding and thrusting, and finally the Montbéliard Plateau, that is primarily affected by normal faulting. Note that the Ognon Fault farther to the north represents a normal fault, with only minor presumed thick-skinned Neogene to recent reactivation; it forms the eastern continuation of the Avant-Monts Fault, reactivated by compression later (see Figure 8c). (b) Section BB′ crosses the Besançon Zone near borehole Chailluz (Ch; Figures 5 and 6) where the thin-skinned Jura fold-and-thrust belt propagated north beyond the Faisceau Bisontin, i.e., the eastern continuation of the Faisceau Lomont in section AA′A″. Note the presence of normal faults of Paleozoic and/or Paleogene age underlying the thrusted Mesozoic sediments, most importantly underneath the Chailluz Anticline and the Faisceau Bisontin, where they controlled the nucleation of fault-related folds during thin-skinned tectonics. (c) Section CC′ traverses the Avant-Monts Zone, bordered to north by the western segment of the Avant-Monts Fault representing a steep reverse fault, as imaged by the Moutherot well and seismic reflection data (Figures 5, 6, and 7). The reverse fault formed by inversion of a Paleogene graben, inferred to have formed along the eastern continuation of the La Serre Horst. Deformation is thick-skinned since the fault dissects the evaporitic décollement level of the thin-skinned Jura fold-and-thrust belt located farther south. The geometry of the latter is again controlled by NNS–SSE striking Paleozoic and/or Paleogene normal faults that control the location of the front of the Besançon Zone and the Faisceau Bisontin.

Bresse Transfer Zone, (3) minor NE–SW directed shortening of probably early Miocene age, and (4) overall NW–SE shortening of late Miocene to recent age related to the Alpine collision.

[42] A discussion of the entire paleostress data set and the complete deformation sequence in the study area is beyond the scope of this presentation. The reader is referred to previous investigations mentioned above and to further discussions of *Madritsch* [2008] regarding our working area. Here we concentrate on the latest, i.e., the late Miocene to recent deformation event. Attributing fault slip data sets to a specific event is difficult, especially in the area

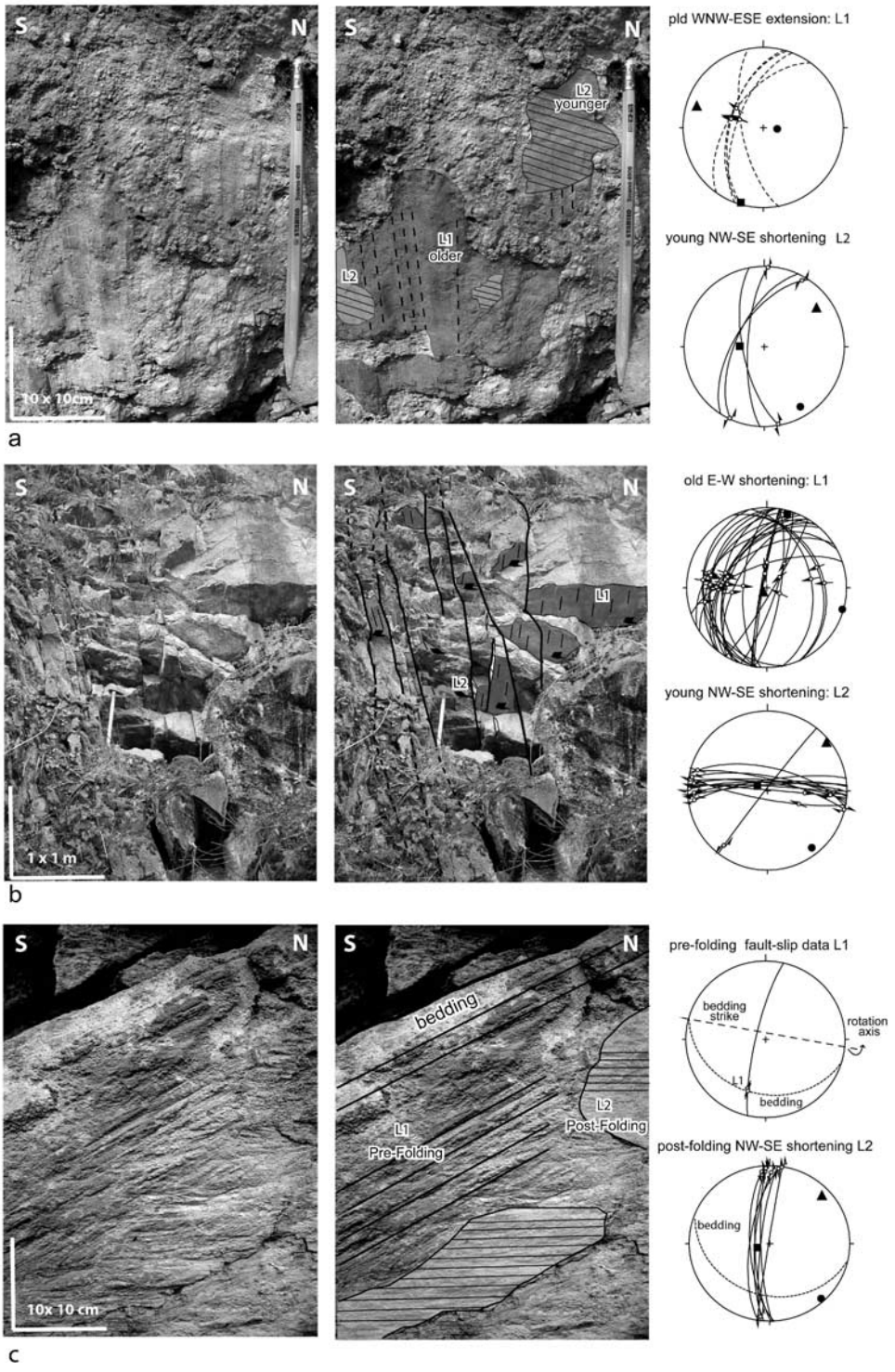

Figure 9

of investigation where all fault slip data were collected in Mesozoic rocks and where no stratigraphic age control is available. However, field observations such as overprinting criteria between differently oriented striations on one and the same fault plane (Figure 9a), crosscutting relationships between different and kinematically incompatible fault planes (Figure 9b), and finally, rotation of fault slip pairs in folded areas (Figure 9c) enabled for establishing a relative chronology of the deformation events observed that could be correlated with that established for neighboring areas [*Bergerat*, 1987; *Lacombe et al.*, 1993; *Homberg et al.*, 1999; *Lacombe and Obert*, 2000; *Homberg et al.*, 2002; *Rocher et al.*, 2003].

[43] Of particular importance for the purpose of this study is the distinction between strike-slip fault sets that are related to an early Eocene and so-called "Pyrenean" event [*Letouzey*, 1986; *Bergerat*, 1987] on one side from those that are related to early Miocene to recent structures formed in the context of the Alpine collision and the formation of the Jura fold-and-thrust belt, on the other side. Structures related to the latter, i.e., the late Miocene to recent deformation events, can be identified as they commonly overprint normal faults related to the prominent Eo-Oligocene extension that led to the formation of the Rhine-Bresse Transfer Zone (Figure 9a) [*Bergerat*, 1987; *Lacombe et al.*, 1993]. Furthermore, in folded areas the relative age of fracture development and related stress regime with respect to folding may be obtained [*Homberg et al.*, 1999] (Figures 9c and 10). In most cases stresses within the crust fulfill the Andersonian law [*Anderson*, 1942; *Brudy et al.*, 1997] that predicts two horizontally and one vertically orientated principal stress axes. If this is not the case the fault set has been tilted after its formation, provided it formed near the earth's surface. In such cases none of the principal stress axes are vertical and two axes lie within the inclined bedding plane [*Homberg et al.* 1999] (Figure 10). Rotated fault slip data sets and related paleostress axes fulfill the Andersonian model after back tilting along the strike of the bedding plane by the amount of bedding dip (Figure 10). This criterion has already been successfully applied throughout the internal Jura fold-and-thrust belt in order to distinguish between prefolding and postfolding faulting events [*Homberg et al.*, 1999, 2002].

[44] In this study more than 1600 fault slip pairs have been collected from 77 locations. The data set and the results of the paleostress analysis are given in Table 1 and are displayed in Figures 11 and 12 in the form of a stress tensor map and related stereo plots. All measurements, with a few exceptions only (sites 12, 69, 70, 73), were taken in Middle (Bathonian to Bajocian) or Late Jurassic (Oxfordian

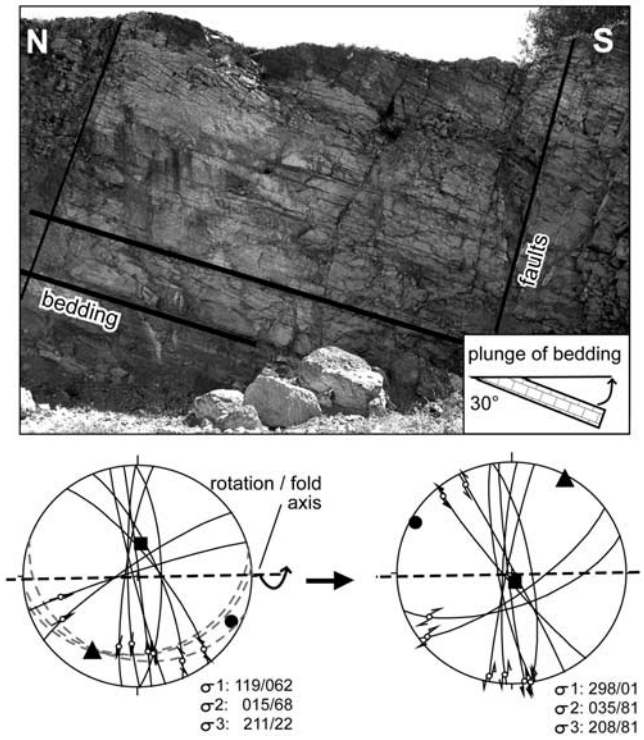

Figure 10. Faulting-folding relationships observed along the thick-skinned Moutherot Anticline. Latest stage folding is recorded by the tilting of the youngest fault set observed throughout the area, defining the widespread NW–SE trending "Alpine" compression. The tilting is evident from the orientation of the paleostress axes prior and after back tilting along a rotation axis parallel to the bedding strike (black dashed line) by the amount of the dip of the bedding. Faults are shown in stereographic lower hemisphere equal-area projections; circles, squares, and triangles mark the maximum, intermediate, and minimum axes of incremental stress, respectively.

Figure 9. Examples of polyphase brittle structures. Faults are shown in stereographic lower hemisphere equal-area projections; circles, squares, and triangles mark the axes of maximum, intermediate, and minimum axes of principal stress, respectively. (a) Overprinting criteria testify for fault reactivation and enable establishment of a relative chronology between different slip events on the same fault plane. Slickolites formed by NW–SE directed extension (dashed lines) are overprinted by younger subhorizontal strike-slip-related slickolites (underlined by solid lines). The latter indicate NW–SE directed compression. (b) Crosscutting criteria allow distinguishing between different fault sets; low-angle reverse faults are systematically crosscut and dissected by steep strike-slip faults. While the reverse faults record E–W contraction, the strike-slip faults document younger and NW–SE directed contraction. (c) Relative chronology of brittle faulting, as inferred from relations between Neogene faulting and folding. Prefolding striations L1 became rotated during folding and need to be rotated back to their former position by the amount of bedding dip and around a rotation axis parallel to the strike of bedding before inferring paleostress. A new generation of fault slip striations L2 overprints the rotated striations and shows no signs of rotation by folding. While folding occurred under NS contraction in this area, postfolding striations indicate younger NW–SE contraction.

Table 1. Results of the Paleostress Analysis[a]

No.	Locality	X	Y	Age	Tectonic Unit	σ1		σ2		σ3		Φ	Tectonic Regime	N	n	Quality	Rot.
						Azi	Pl	Azi	Pl	Azi	Pl						
1	Bart	933869	2285000	Rauracien	Montbéliard Plateau	320	1	76	87	230	2		strike-slip	14	0	2	x
2	Mont Bart	933420	2286010	Sequanien	Montbéliard Plateau	330	1	81	87	240	3		strike-slip	24	0	1	x
3a	Bavans	932186	2285113	Bajocien	Montbéliard Plateau	6	7	96	1	193	82		reverse	13	1	1	
3b	Bavans	932186	2285113	Bajocien	Montbéliard Plateau	141	11	270	73	49	13	0.47	strike-slip	17	1	1	
4	Colombiere Fontaine	928370	2281073	Sequanien	Montbéliard Plateau	335	5	160	85	65	0		strike-slip	14	0	1	
5	Longevelle	926463	2281522	Sequanien	Montbéliard Plateau	149	9	292	79	58	6		strike-slip	26	2	1	
6	Longevelle West	923433	2281634	Sequanien	Montbéliard Plateau	159	5	272	77	68	12	0.48	strike-slip	28	1	1	
7	L'Isle sur le Doubs	920067	2281297	Rauracien	Montbéliard Plateau	147	7	272	78	56	10		strike-slip	19	0	2	
8a	Anteuil	917598	2273891	Bathonien	Besançon Zone	184	1	276	76	94	14	0.37	transpressional	36	3	1	
8b	Anteuil	917598	2273891	Bathonien	Besançon Zone	142	1	48	78	232	12	0.47	strike-slip	14	0	3	
9	Clerval	914680	2273779	Bajocien	Besançon Zone	170	3	272	75	79	15	0.28	transpressional	23	5	1	
10	L'Hopital St. Lieffroy	912212	2275014	Sequanien	Montbéliard Plateau	322	0	53	87	232	3		strike-slip	21	1	1	
11	Soye	913222	2279839	Callovien	Montbéliard Plateau	334	3	100	85	244	4		strike-slip	10	0	1	
12	Vellechevreux	915862	2290580	Middle Triassic	Montbéliard Plateau	155	2	258	80	65	10		strike-slip	5	1	2	
13	Gouhenans	910304	2297344	Bajocien	Vesoul Plateau	157	5	286	82	66	6		strike-slip	13	4	3	
14	Aillevans	906601	2296221	Bajocien	Vesoul Plateau	151	5	25	81	242	7		strike-slip	24	3	2	
15	Vergranne	904581	2280288	Bathonien	Montbéliard Plateau	122	7	349	80	213	7		strike-slip	22	8	1	
16	Romain	904581	2280288	Bathonien	Montbéliard Plateau	333	1	73	85	243	5		strike-slip	41	6	1	
17	Montagney-Servigney	899644	2283654	Sequanien	Vesoul Plateau	165	1	267	86	75	4		strike-slip	16	6	3	
18	Cognieres	896726	2285000	Sequanien	Vesoul Plateau	165	13	11	75	257	6	0.5	strike-slip	14	0	1	
19	Fontenois les Montbozon	894370	2282868	Sequanien	Vesoul Plateau	305	1	47	83	215	7		strike-slip	11	5	2	
20	Tallans	904918	2275125	Bajocien	Montbéliard Plateau	337	7	149	83	247	1		strike-slip	8	1	3	
21	Battenans les Mines	898858	2276809	Bajocien	Vesoul Plateau	163	2	33	87	253	3		strike-slip	9	3	3	
22	Ormenans	897288	2274789	Sequanien	Vesoul Plateau	349	2	94	82	258	8		strike-slip	20	5	1	
23	Germondans la Roche	891340	2274340	Sequanien	Vesoul Plateau	138	3	35	75	229	15	0.52	strike-slip	11	2	1	
24	Rigney la Roche	891000	2273891	Sequanien	Vesoul Plateau	154	4	292	85	64	4		strike-slip	16	9	2	
25	Baume-les-Dames East	905703	2268393	Bajocien	Faisceau Bisontin	138	2	34	82	228	8		strike-slip	21	4	1	
26	Baume-les-Dames	901103	2268729	Bajocien	Besançon Zone	344	8	193	81	74	4		strike-slip	14	0	1	x
27	Champlive	895267	2262445	Bajocien	Faisceau Bisontin	332	2	224	83	62	7		strike-slip	8	4	3	x
28	Deluz	891228	2262558	Callovien	Besançon Zone	318	0	226	87	48	3		strike-slip	14	0	2	x
29	Amagney	888759	2662445	Rauracien	Besançon Zone	152	4	314	86	62	1		strike-slip	18	5	2	
30	Chaudefontaine	8888871	2263680	Callovien	Besançon Zone	147	10	316	80	56	2		strike-slip	22	8	2	
31	Tratiefontaine	884495	2275013	Sequanien	Vesoul platform	313	2	138	88	43	0		strike-slip	7	5	2	
32	Marchaux	885618	2265475	Bathonien	Besançon Zone	307	5	64	79	216	10		strike-slip	43	13	2	
33	Boult	877201	2270637	Rauracien	Vesoul Plateau	174	6	58	76	266	12	0.54	strike-slip	18	1	2	
34	Besancon	896165	2259079	Bathonien	Besançon Zone	310	3	172	86	41	3		strike-slip	27	7	1	
35	Tallenay	879221	2262109	Bajocien	Besançon Zone	322	12	125	77	231	4		strike-slip	6	2	3	x
36	Devecey	875967	2262445	Bajocien	Besançon Zone	350	0	260	67	81	23	0.37	transpressional	16	4	3	
37	Auxon-Dessus	875743	2262333	Bajocien	Besançon Zone	138	6	241	65	45	24	0.37	transpressional	17	0	1	
38	Besancon/Temis	876865	2256723	Bajocien	Besançon Zone	139	5	36	68	231	21	0.38	transpressional	36	11	1	
39	Besancon/St.Léonard	881017	2253518	Sequanien	Faisceau Bisontin	357	10	264	13	124	74	0.49	reverse	7	0	2	
40	Chaudanne	878436	2254142	Bathonien	Besançon Zone	330	13	62	10	188	73	0.32	transpressional	21	2	1	
41	Beure	878099	2252458	Rauracien	Faisceau Bisontin	144	7	282	80	53	7		strike-slip	39	9	1	
42	Arguel	877987	2251224	Sequanien	Faisceau Bisontin	165	5	74	3	313	84		reverse	34	7	1	
43	Pugey	877762	2247970	Bajocien	Faisceau Bisontin	128	5	281	84	38	3		strike-slip	10	3	3	
44	Epeugney	878548	2246062	Bathonien	Faisceau Bisontin	117	3	7	83	207	7		strike-slip	18	3	2	
45	Planoise	875855	2251336	Bajocien	Besançon Zone	327	11	155	78	57	2		strike-slip	17	1	1	
46	Rancenay	874284	2249653	Bathonien	Besançon Zone	166	5	281	79	75	10		strike-slip	12	2	2	x

Table 1. (continued)

No.	Locality	X	Y	Age	Tectonic Unit	σ1		σ2		σ3		Φ	Tectonic Regime	N	n	Quality	Rot.
						Azi	Pl	Azi	Pl	Azi	Pl						
47	Busy	874733	2247858	Bajocien/	Faisceau Bisontin	320	14	228	9	106	73	0.36	transpressional	28	0	1	
48	Bussieres	870356	2246736	Bajocien	Besançon Zone	141	1	288	89	51	1		strike-slip	13	3	2	
49	Routélle	866878	2245389	Bajocien	Besançon Zone	333	4	81	78	242	11	0.49	strike-slip	10	1	1	x
50	Abbans Dessous	868673	2240676	Bajocien	Besançon Zone	160	11	273	64	66	23	0.49	strike-slip	10	3	2	
51	Quingey	870693	2239788	Bathonien	Faisceau de Quingey	132	6	16	77	224	12	0.26	transpressional	47	0	1	
52	Pointvillers	870132	2236637	Portlandien	Faisceau de Quingey	306	11	117	79	216	2		strike-slip	34	2	1	
53a	Ivrey	871478	2227659	Bajocien	Faisceau de Quingey	106	2	16	5	215	84		reverse	25	0	1	
53b	Ivrey	871478	2227659	Bajocien	Faisceau de Quingey	142	10	294	79	51	5		strike-slip	14	1	1	
54	St. Jospeh	866890	2224486	Portlandien	Faisceau de Quingey	289	1	126	87	19	1		strike-slip	16	3	3	
55	Port Lesney	863736	2229006	Rauracien	Faisceau de Quingey	133	x	24	83	223	8		strike-slip	7	2	3	
56	Pin	865868	2265924	Sequanien	Vesoul Plateau	169	1	30	88	259	1		strike-slip	11	4	2	
57	Chaucenne	869907	2259640	Sequanien	Besançon Zone	101	2	8	63	192	27	0.43	strike-slip	7	0	3	
58	Champagney	869795	2255489	Aalenien	Besançon Zone	344	9	146	81	250	2		strike-slip	9	1	2	
59	Chemaudin	869683	2251673	Bathonien	Besançon Zone	112	7	339	80	203	7		strike-slip	44	7	2	
60	St. Vit	865082	2248531	Bathonien	Besançon Zone	126	2	13	86	216	4		strike-slip	24	11	2	
61	Fraisans	860033	2243930	Rauracien	Avant-Monts Zone	308	4	69	82	217	7		strike-slip	8	2	3	
62	Ranchot	837564	2244604	Bathonien	Avant-Monts Zone	150	2	311	88	60	1		strike-slip	8	4	1	
63	Monteplain	855656	2244379	Callovien	Avant-Monts Zone	167	12	5	76	256	3	0.54	strike-slip	31	4	2	
64	Marnay	857676	2261435	Rauracien	Vesoul Plateau	325	15	115	73	233	8	0.5	strike-slip	20	8	1	
65	Montagney	852290	2258967	Sequanien	Vesoul Plateau	299	5	45	74	208	15	0.44	strike-slip	12	2	3	
66	Taxenne	853637	2252571	Bajocien	Avant-Monts Zone	295	13	171	65	30	19	0.59	strike-slip	14	5	1	x
67	Gendrey	852178	2251000	Bathonien	Avant-Monts Zone	118	2	223	82	28	7		strike-slip	75	28	3	
68	Orchamps	849709	2243594	Bathonien	Avant-Monts Zone	327	1	220	88	57	2		strike-slip	36	20	1	
69	Forêt de la Serre	844772	2247072	Paleozoic Granite	Avant-Monts Zone	330	7	81	71	238	17	0.46	strike-slip	18	8	1	
70	Moissey	843650	2249429	Permian Vulcanite	Avant-Monts Zone	333	7	181	82	64	4		strike-slip	27	7	2	
71	Peintre	839722	2248756	Bathonien	Vesoul Plateau	300	14	189	56	38	30	0.51	strike-slip	23	1	2	
72	Amange	844435	2246175	Bajocien	Avant-Monts Zone	340	7	82	61	246	28	0.53	strike-slip	15	6	3	
73	Jouhe	839834	2242920	Aalenien	Avant-Monts Zone	151	5	260	76	60	13	0.46	strike-slip	12	6	1	
74	Authume	839385	2239778	Bathonien	Avant-Monts Zone	152	6	31	78	243	10		strike-slip	35	18	1	
75	Mont Roland	837702	2239442	Bathonien	Avant-Monts Zone	156	5	45	75	247	14	0.55	strike-slip	26	12	1	
76	Monniere	837702	2238544	Bajocien	Avant-Monts Zone	140	10	25	68	234	20	0.46	strike-slip	18	3	1	
77	Dampiere	834224	2234180	Sequanien	Avant-Monts Zone	148	6	51	52	243	37	0.32	transpressional	20	3	1	

[a]Numbers refer to Figures 10 and 11. Coordinates (X/Y) given in meters (France II Lambert Conformal Conic system); σ1, σ2, σ3, maximum, intermediate, and minimum principal stress axes; Azi, azimuth; pl, plunge; N, number of fault slip pairs considered for paleostress calculation; n, number fault slip pairs with no indication of slip direction; Φ, stress ration from NDA paleostress calculation indication the tectonic regime (Φ ∼ 0.25 transpression; Φ ∼ 0.5 reverse/strike-slip faulting compare Figure 12); quality: 1 excellent, 2 good, 3 poor.; Rot, data sets that were inferred to be tilted and back rotated before paleostress calculation (compare Figure 10).

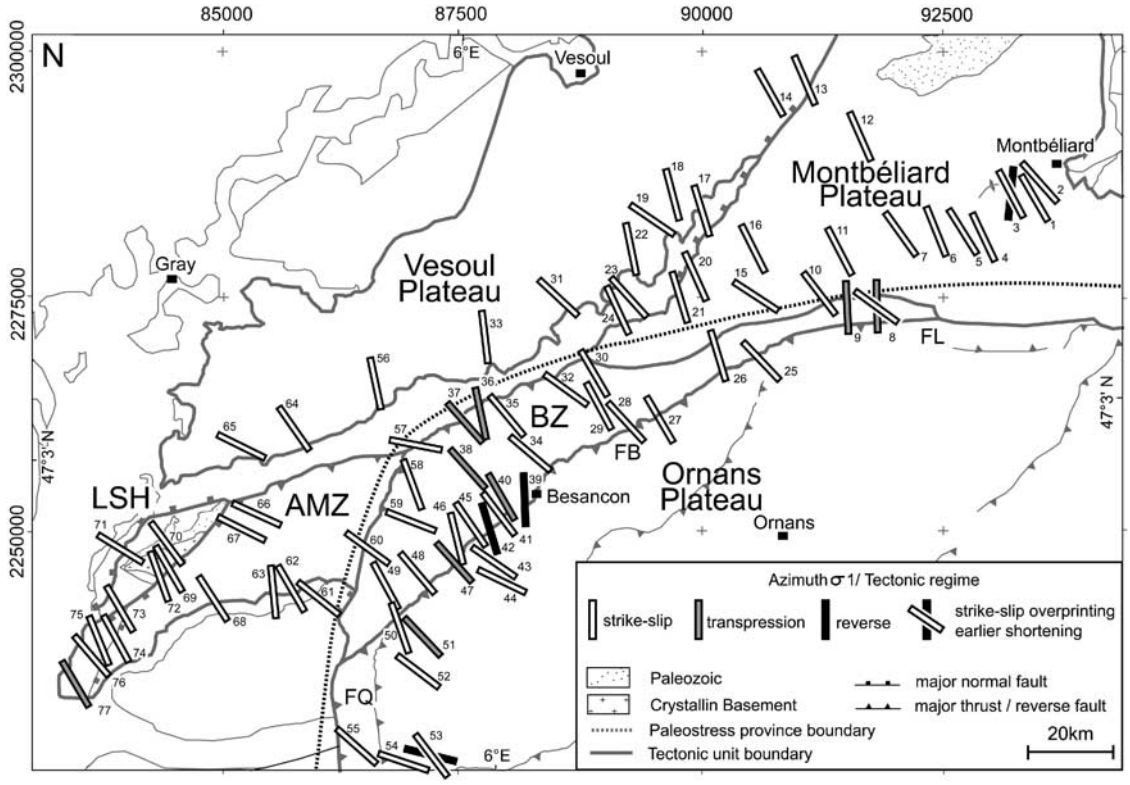

Figure 11. Map showing the azimuth (bars) of the axes of maximum principal stress ($\sigma 1$), superimposed on a schematic version of the structural map of the study area presented in Figure 3. Numbers next to the bars, given in different gray tone depending on the tectonic regime, refer to Table 1 and Figure 12. The stippled line marks the boundary between two paleostress provinces (see text for discussion). AMZ, Avant-Monts Zone; BZ, Besançon Zone; FB, Faisceau Bisontin; FL, Faisceau du Lomont; FQ, Faisceau de Quingey; LSH, La Serre Horst.

to Kimmeridgian) limestones. Slickolites were the most frequently available sense of slip indicators; calcite slickenfibres and lunate fractures [*Petit*, 1987] were also used. The kinematic indicators were ranked according to quality from 1 (excellent) to 3 (poor) (see Table 1). Bedding was subhorizontal at most sites investigated during this study. At localities where the inclination of the bedding exceeded 20° its orientation is indicated in Figure 12 (dashed gray lines). Fault sets that were interpreted to have been tilted by folding and were back-rotated prior to paleostress calculations (Figure 10) and are noted in Table 1.

[45] The field data were processed with the Windows-based computer program TectonicsFP (F. Reiter and P. Acs, TectonicsFP, Innsbruck, Computer Software for Structural Geology, version 2.0 PR, 1996–2000, available at http://www.tectonicsfp.com/). Data sets from each locality were separated into homogenous subsets, based on overprinting and/or or crosscutting criteria. In addition we applied the pole projection plot [*Meschede and Decker*, 1993] and the p-t axes method [*Marrett and Allmendinger*, 1990] in order to graphically test the fault sets for kinematic homogeneity [*Madritsch*, 2008]. Thereby incompatible fault-striation pairs within a given subset were detected and reconsidered as being part of another subset by additionally taking into account the quality of the slip indicator. The Right-Dihedra method [*Angelier and Mechler*, 1977; *Pfiffner and Burkhard*, 1987] was then used for calculating the orientation of the principal stress axes ($\sigma 1 > \sigma 2 > \sigma 3$). The comparison of the results of the kinematic p-t axes with those obtained by the dynamic Right-Dihedra method in this study revealed similar results. The orientation of incremental strain and the principal stress axes coincided, which indicates coaxial deformation.

[46] The orientation of these axes yields the tectonic regime at any given location. In this contribution we do not discuss extensional and transtensional stress states that occur widespread throughout the area but which are related to older, i.e., post-Jurassic to Eo-Oligocene deformation

Figure 12. Stereographic lower hemisphere equal-area projection of fault slip data obtained in the study area and results of the Right-Dihedra paleostress determination. Circles, squares, and triangles mark the maximum, intermediate, and minimum principal stress axes, respectively (see Table 1 and Figure 11 for details and the location of observation points). Dashed gray lines mark the bedding orientation were inclined more than 20°.

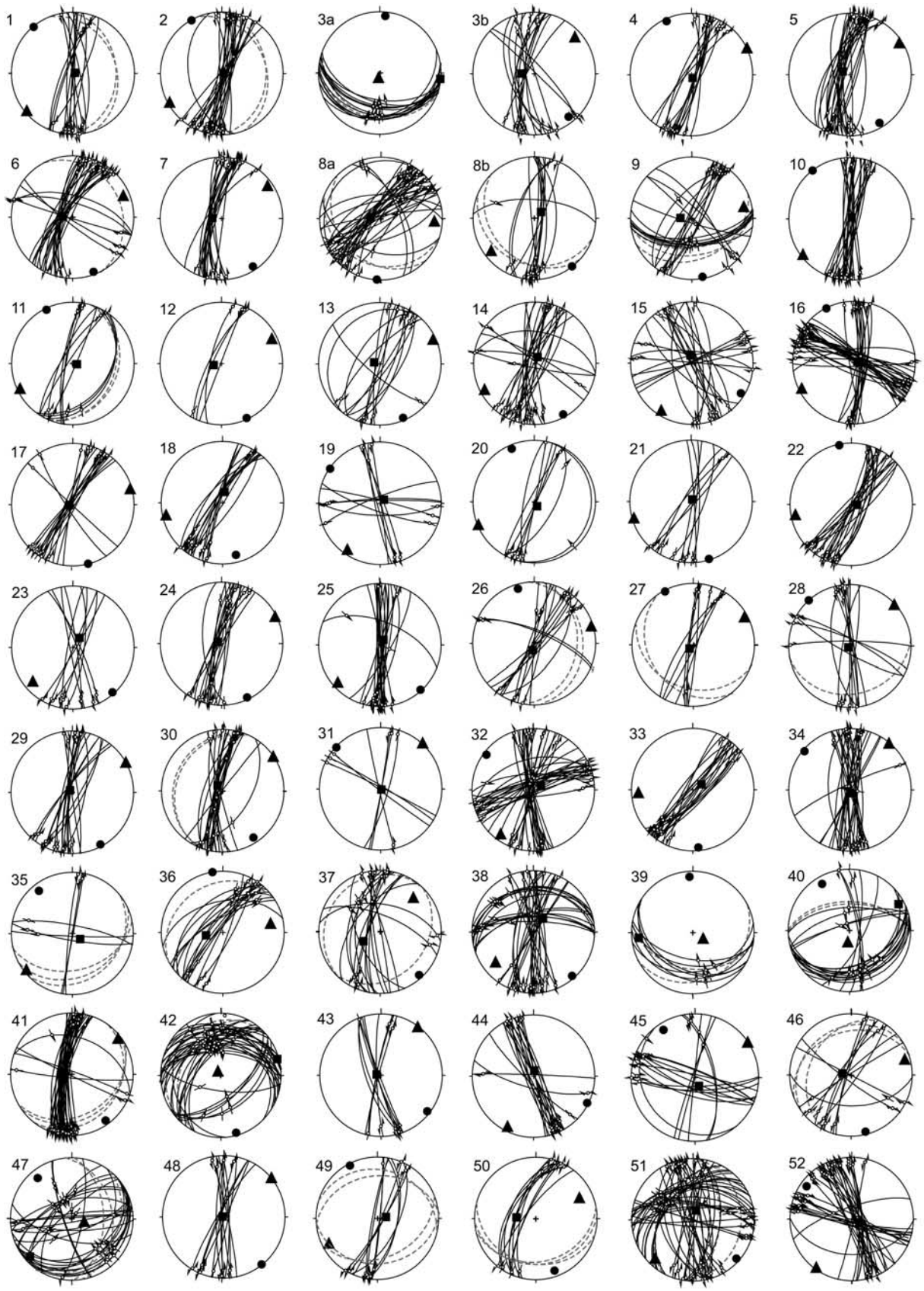
1
2
3a
3b
4
5
6
7
8a
8b
9
10
11
12
13
14
15
16
17
18
19
20
21
22
23
24
25
26
27
28
29
30
31
32
33
34
35
36
37
38
39
40
41
42
43
44
45
46
47
48
49
50
51
52

Figure 12

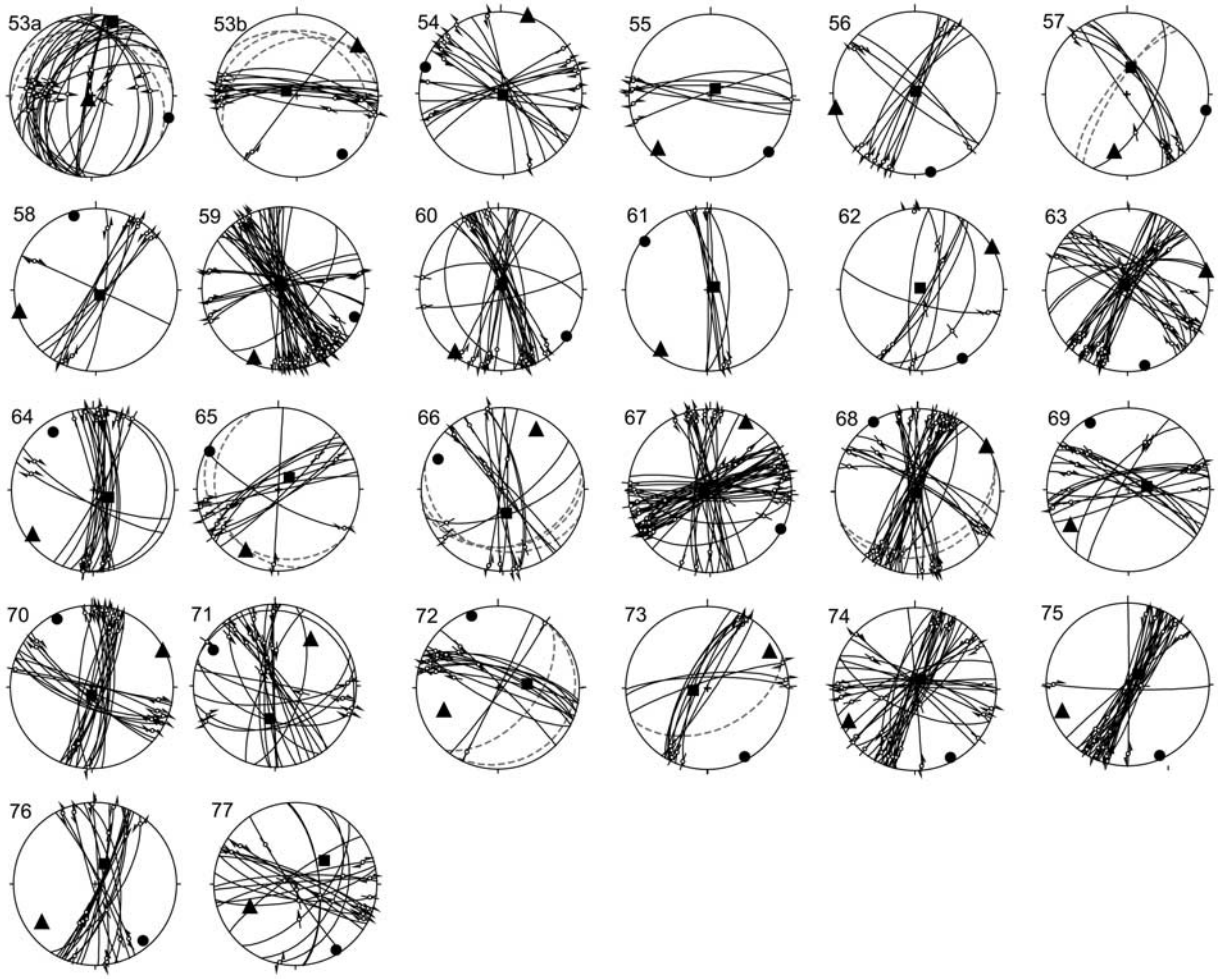

Figure 12. (continued)

events [see *Letouzey*, 1986; *Bergerat*, 1987; *Lacombe et al.*, 1993; *Rocher et al.*, 2003; *Madritsch*, 2008]. Concentrating on the overall NW–SE shortening of late Miocene to recent age related to the Alpine collision we only distinguish between reverse faulting ($\sigma1$ horizontal, $\sigma3$ subvertical, well defined point maxima of p and t axes) and strike-slip faulting ($\sigma1$ and $\sigma3$ horizontal, well defined point maxima of p and t axes). Furthermore, intermediate cases of transpression ($\sigma1$ horizontal, $\sigma2$ and $\sigma3$ ill defined, p axes clustered around a point maximum, great circle distribution of t axes) were observed at sites where kinematically compatible reverse and strike-slip faults coexist in the absence of crosscutting or other overprint criteria (e.g., sites 36, 37, and 38, Table 1). As the Right-Dihedra method does not yield the stress ratio ($\Phi = (\sigma2 - \sigma3)/(\sigma1 - \sigma3)$) such intermediate stress states are ill defined. In questionable cases, i.e., when $\sigma3$ exhibits a significant plunge (10–80°), we additionally performed a numeric-dynamic paleostress calculation applying the NDA method [*Spang*, 1972; *Sperner et al.*, 1993] (noted in Table 1). The results of this paleostress calculation were always in good agreement with the Right Dihedra method and yielded the stress ratio (Φ) in order to unambiguously define such intermediate tectonic regimes (transpression, $\Phi \sim 0.25$; reverse and strike-slip faulting, $\Phi \sim 0.5$).

3.3.2. Results

[47] The paleostress analysis indicates that the overall Neogene to recent maximum horizontal stress is oriented NW–SE throughout the area (Figures 11 and 12). This is in agreement with former studies from neighboring areas that applied Direct Inversion methods [*Bergerat*, 1987; *Lacombe et al.*, 1993; *Homberg et al.*, 2002]. Subtle variations in the orientation of paleostress axes, especially the azimuth of the maximum principal stress axis ($\sigma1$), and different types of outcrop-scale brittle structures observed at the various sites, allow for a distinction between an internal and an external paleostress province (Figures 11 and 13). The former comprises the areas governed by thin-skinned deformation, the latter is located north and northwest of the front of the thin-skinned fold-and-thrust belt, comprising the areas of the foreland that are partly affected by thick-skinned deformation.

[48] The internal paleostress province, characterized by a thin-skinned deformation style, extends along the Lomont,

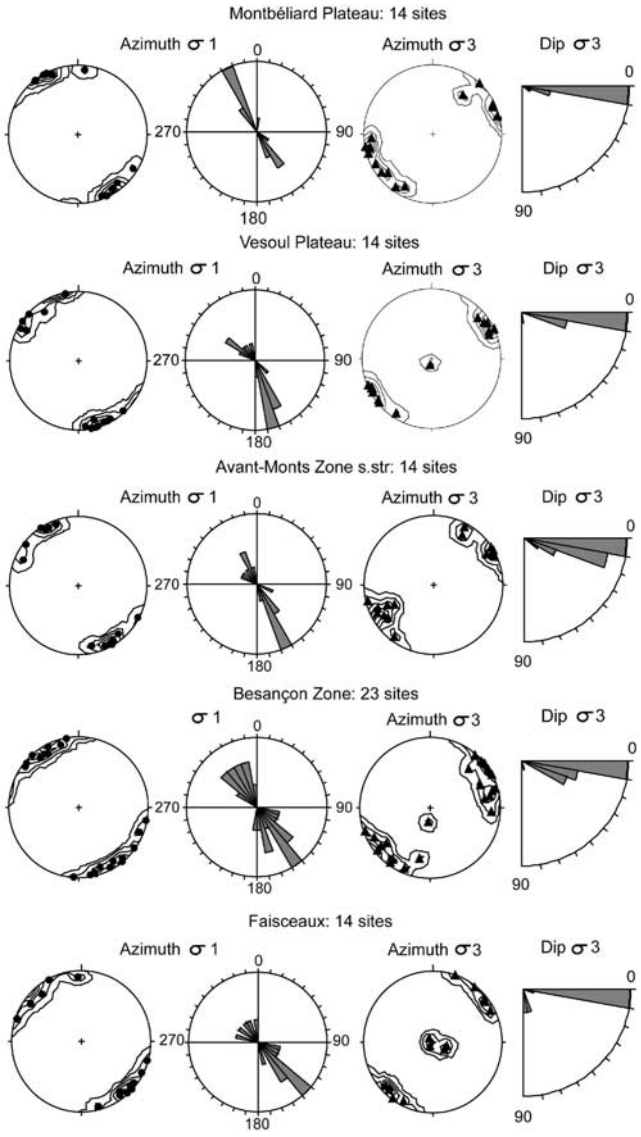

Figure 13. Directional analysis of calculated paleostress axes for the various tectonic units. From left to right, contoured plot of $\sigma 1$; rose diagram of the azimuth of $\sigma 1$; contoured plot of $\sigma 3$, and inclination diagram of the plunge of $\sigma 3$ (lower hemisphere stereographic equal-area projection). The Montbéliard and Vesoul plateaux, as well as the Avant-Monts Zone, comprise an external paleostress province (Figure 10) characterized by a uniform direction of $\sigma 1$ striking NW–SE and by a close to horizontally oriented $\sigma 3$. By contrast, the orientation of $\sigma 1$ within in the internal paleostress province, comprising the Besançon Zone and the Lomont, Bisontin, and Quingey faisceaux, has a tendency for fanning, while $\sigma 3$ is close to vertical at many of the studied sites.

Bisontin, and Quingey faisceaux and the Plateau Jura proper and also includes the Besançon Zone. Throughout this province the orientation of the maximum principal stress axes ($\sigma 1$) undergoes a discernible and systematic change in orientation (Figures 11 and 13): $\sigma 1$ strikes N–S in the east, gradually turns over a to a NW–SE orientation farther west, and finally into the WNW–ESE direction observed in the southwest. This fanning stress pattern was also noted by previous authors [e.g., *Laubscher*, 1972; *Homberg et al.*, 1999, 2002] and represents a typical phenomenon associated with the thin-skinned tectonics of the arcuate thin-skinned Jura fold-and-thrust belt [*Philippe et al.*, 1996; *Hindle and Burkhard*, 1999; *Affolter and Gratier*, 2004].

[49] The stress trajectories in the internal paleostress province are most often defined by steep conjugate strike-slip faults that define a strike slip tectonic regime (white arrows, $\sigma 1$ and 3 horizontal $\sigma 2$ vertical) (Figures 11 and 12). Almost everywhere such strike-slip faults were found to overprint and reactivate older preexisting normal faults or extension gashes (Figure 9a). The latter are interpreted as having formed during the prominent Eo-Oligocene extension [*Lacombe et al.*, 1993; *Madritsch*, 2008]. In the eastern part of the study area, where strike-slip faults indicate N–S directed stress orientations similar to those related to the "Pyrenean" shortening of presumably early Eocene age [*Bergerat*, 1987; *Homberg et al.*, 2002], overprinting criteria in respect to Eo-Oligocene extensional structures provide the main criterion for their attribution to Neogene age deformation. Moreover, in areas affected by Neogene folding these fault sets are strictly perpendicular to the trend of the Neogene thrust faults and fold axes, which makes their attribution to Neogene deformation even more likely (Figures 11 and 14).

[50] At some localities, near the major deformation fronts of the Faisceau du Lomont, Bisontin and Quingey or, alternatively, at the northern rim of the Besançon Zone, shortening is taken up by low-angle thrust faults that define a tectonic regime of reverse faulting (Figures 11 and 12, e.g., sites 39, 40, and 53). These faults consistently developed during a late stage of folding (Figure 14). At other sites, mostly located at the northwestern rim of the Besançon Zone, an intermediate tectonic regime of transpression was inferred (gray arrows in Figure 11, e.g., sites 36, 37, 38, and 50). Throughout the Jura fold-and-thrust belt, a tectonic regime characterized by permutations of $\sigma 2$ and $\sigma 3$ was found to be typical for areas characterized by tear faults and lateral ramps [*Laubscher*, 1972; *Homberg et al.*, 2002; *Ustaszewski and Schmid*, 2006].

[51] Differing paleostress axis orientations at a given locality could, in many places, be explained by strain partitioning controlled by the availability of preexisting normal faults, and could hence be theoretically related to a unique tectonic event. However, there are some key outcrops where systematic overprinting relationships between two separate Neogene deformation phases of different orientation were observed. At site 53 along the Faisceau de Quingey, top-to-the-west low-angle thrust faults, which reflect E–W shortening, are overprinted by strike-slip faults that yield NW–SE shortening (Figure 9b). Another evidence is provided at locations 3, 8, and 9 north of the Faisceau du Lomont (Figure 11), where N–S striking strike-slip faults indicating NW–SE directed shortening are seen to postdate N–S directed shortening related to the folding of

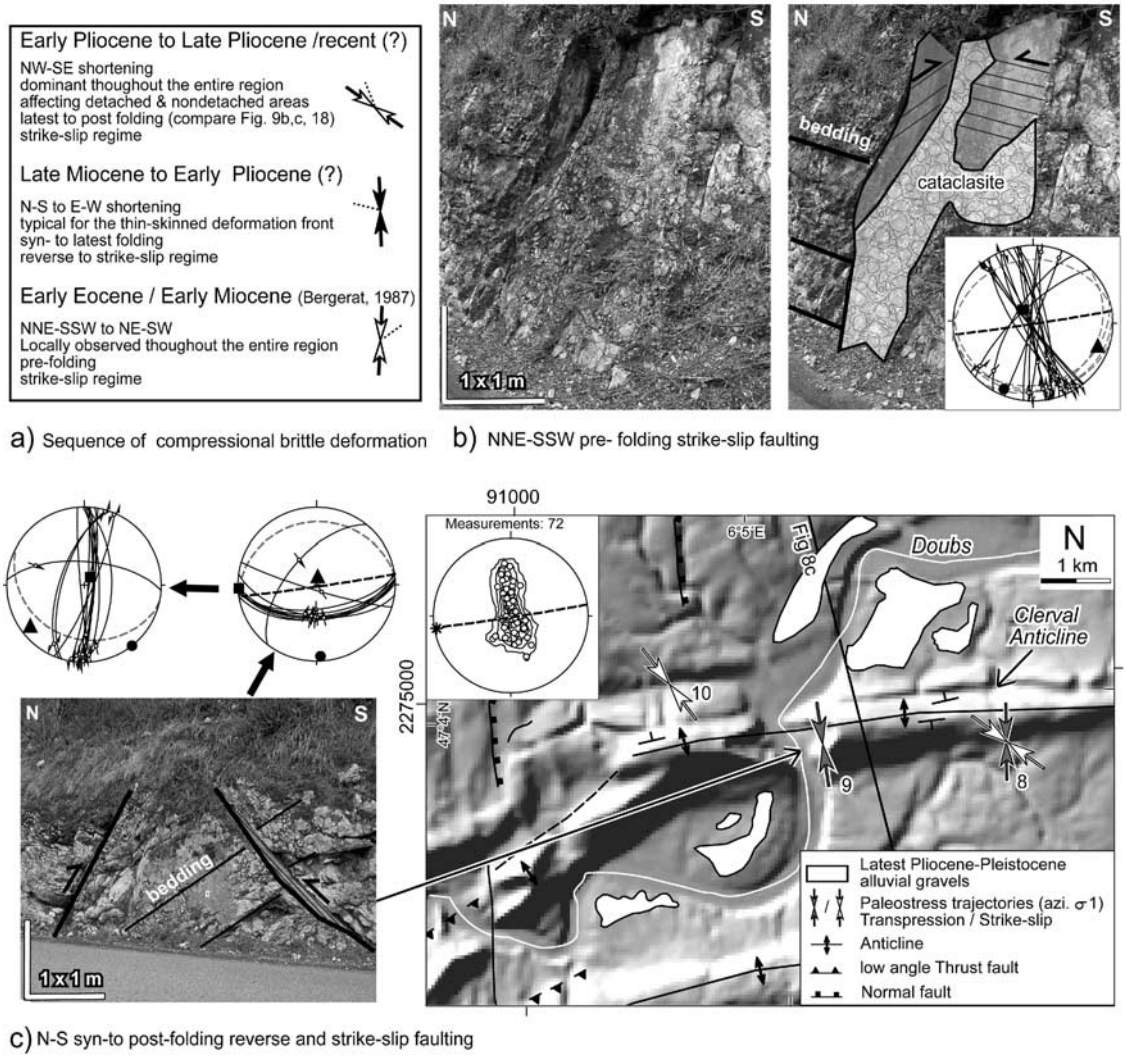

Figure 14. Faulting and folding relationships observed along the Clerval Anticline (see Figure 3 for location). Fault slip data are displayed in form of stereographic lower hemisphere equal-area projection; $\sigma 1$, $\sigma 2$, and $\sigma 3$ are shown by circles, squares, and triangles, respectively. Gray dashed lines show the orientation of bedding. (a) Succession of brittle deformations with respect to folding. Arrows show the orientation of $\sigma 1$ as observed at the site, and stippled lines show regional variations. (b) Early stage strike-slip faults slightly tilted by folding. (c) Shaded digital elevation model of the Clerval Anticline (horizontal resolution 50 m). Synfolding to postfolding low-angle thrust faults are observed in the core of the anticline, confining N–S shortening perpendicular to the fold axis. The youngest fault sets comprise strike-slip faults, confining NW–SE shortening oblique to the fold axis (compare Figures 9b and 9c for relative age criteria). Also note the antecedent post-2.9 Ma course of the Doubs River with respect to the fold structure and the distribution of terraces derived from the eroded Sundgau and Forêt de Chaux gravels.

the Clerval and Montbéliard Anticlines (Figures 3, 8a, 9c, and 14). Hence the fanning stress trajectories observed along the Quingey and Bisontin faisceaux appear to be overprinted by consistently NW–SE oriented paleostress trajectories.

[52] These combined regional observations result in a sequence of compressional brittle deformations that initiated in the late Miocene in this part of the Jura fold-and-thrust belt [*Becker*, 2000; *Ustaszewski and Schmid*, 2006] (Figure 14a). Figure 14 illustrates the situation along the Clerval Anticline that is located at the eastern margin of the study area and north to the Faisceau du Lomont, and is therefore part of the Besançon Zone (Figures 3 and 8a). Toward the west the fold links up with shallow thrust faults. These observations, together with interpretations of seismic reflection data, strongly suggest a thin-skinned formation of

the fold structure, at least during an initial stage, when it probably nucleated along a preexisting normal fault (see interpretation given in Figure 8a).

[53] The earliest compressional structures observed in the Clerval area are strike-slip faults (Figure 14b). The deduced paleostress axes trend oblique to the fold axis. These fault sets are always to some extent affected by folding (Figure 14b), which hints toward a prefolding to synfolding formation. These structures are inferred to have formed in early Eocene (''Pyrenean compression'' [*Bergerat*, 1987]) or, alternatively, in early Neogene times when found to overprint normal faults [*Homberg et al.*, 2002; *Madritsch*, 2008], and they will not be further discussed here. Reverse faults indicate paleostress axes oriented perpendicular to the fold axis, and they dissect the folded beds (Figure 14c). This suggests a synfolding to postfolding age. The youngest fault set comprises strike-slip faults that define NW–SE directed shortening oblique to the fold axis (Figure 14c). As outlined above, these fault sets frequently overprint reverse faults and are hardly affected by folding (Figures 9b and 9c). This is in agreement with observations from the internal Jura fold-and-thrust belt [*Homberg et al.*, 2002].

[54] Unfortunately, overprinting criteria allowing for distinguishing distinct events during the Neogene to recent history of faulting are restricted to areas were stress trajectories related to such different shortening events are oriented at a high angle to each other, which is only the case in the far east and west of the study area (Figure 11). Accordingly, no polyphase overprinting Neogene to recent stress trajectories were detectable in the central part of the study area, e.g., the Besançon Zone, where strike-slip and reverse faults commonly yield parallel shortening directions. Notably, the observation that the youngest recorded fault sets defining NW–SE shortening are not, or hardly, affected by folding does not account for the northern rim of the Besançon Zone. Along the Chailluz Anticline these fault sets are frequently tilted and appear to have formed before or during rather than after folding (Figures 5 and 8b, e.g., site 26, 28, and 35).

[55] The external paleostress province (Figure 11) comprises the Montbéliard and Vesoul plateaus as well as the Avant-Monts Zone. The orientation of $\sigma 1$, as defined by the youngest detected fault sets in this province, scatters slightly between NNW–SSE to WNW–ESE. However, and most importantly, the systematic fanning observed along the front of the thin-skinned thrust belt is not detectable throughout this area (Figures 11 and 13). This is best seen at the northern (sites 4–11, Figure 14) and western (51–55 and 61–63) boundary of the fold-and-thrust belt. In both these areas $\sigma 1$ strikes consistently NW–SE in the external paleostress domain, whereas to the south, and hence within the thin-skinned fold-and-thrust belt, the orientation of $\sigma 1$ is N–S in the eastern part and WNW–ESE in the western part, respectively. The type of rather consistently NW–SE directed stress trajectories is recorded far into the stable foreland NW of the study area [*Bergerat*, 1987; *Lacombe and Obert*, 2000; *Rocher et al.*, 2004].

[56] The stress tensors obtained from the external stress province, similarly to the findings in the internal province, are confined by steep strike-slip faults that reactivated preexisting Paleogene normal faults (Figure 9a). However, low-angle thrust faults are almost nowhere observed in this area. Notable exceptions are site 3 located along the isolated Montbéliard Anticline and sites 71, and 76 from the surroundings of the La Serre Horst (Table 1 and Figures 10 and 11). Regarding temporal relationships between faulting and folding a key observation is shown in Figure 10 where the youngest brittle structures confining NW–SE directed shortening are overprinted by thick-skinned folding along the Moutherot anticline (Figure 10). This argues in favor of a very late stage of thick-skinned folding considering the brittle deformation sequence outlined above (Figure 14).

3.4. Geomorphic Observations

[57] The geomorphology of a region further constrains its tectonic history, provided that sedimentary or morphological deformation markers of known age are available. In intracontinental settings the geometries of fluvial drainage patterns [*Twidal*, 2004] and incision reconstructions of rivers based on stream terraces [*Bull*, 1990; *Merritts et al.*, 1994] may yield information on slow and long-term tectonic processes. Many recent studies have successfully applied such geomorphic approaches in order to study the temporal evolution of fold structures in fold-and-thrust belt settings [*Oberlander*, 1985; *Burbank et al.*, 1996; *Alvarez*, 1999; *Mouthereau et al.*, 2007].

[58] Along the Avant-Monts Fault, where a clear distinction between pure thick-skinned folding along the Moutherot Anticline in the west and predominately thin-skinned deformation along the Chailluz Anticline in the east can be established (Figures 5, 6, 7, 8b, and 8c), geomorphic age constraints are provided by the Plio-Pleistocene evolution and present-day pattern of the drainage system (Figure 15). The area depicted in Figure 15 is characterized by a roughly ENE–WSW trending drainage divide between the drainage areas of the Ognon and the Doubs rivers, both flowing toward the west into the Bresse Graben (BG, see inset in Figure 15). While the main Doubs and Ognon rivers have longitudinal courses that parallel the ENE–WSW striking structural trend, their tributary streams are oriented orthogonally, i.e., in a N–S direction. Note the difference to the drainage pattern of the tributary streams. To the east the drainage divide is very close to the topographic barrier formed by the thin-skinned Chailluz Anticline. Tributary streams reveal a consequent pattern around this anticline [*Twidal*, 2004]. Toward the west, near the transition between Besançon and Avant-Monts Zone, the drainage divide steps back southward and away from the topographic high which evolved via the formation of the thick-skinned Moutherot Anticline. The Ognon tributary river system is antecedent [*Burbank et al.*, 1996; *Alvarez*, 1999] with respect to this fold structure.

[59] The drainage divide between Ognon and Doubs valleys existed from early Pliocene times onward when the two drainage basins were already separated [*Petit et al.*, 1996; *Sissingh*, 2001; *Madritsch*, 2008]. While the Ognon River shed material from the crystalline Vosges mountains (VG, see inset in Figure 15), the precursor of the Doubs River, namely, the Paleo-Aare, shed sediments of Alpine

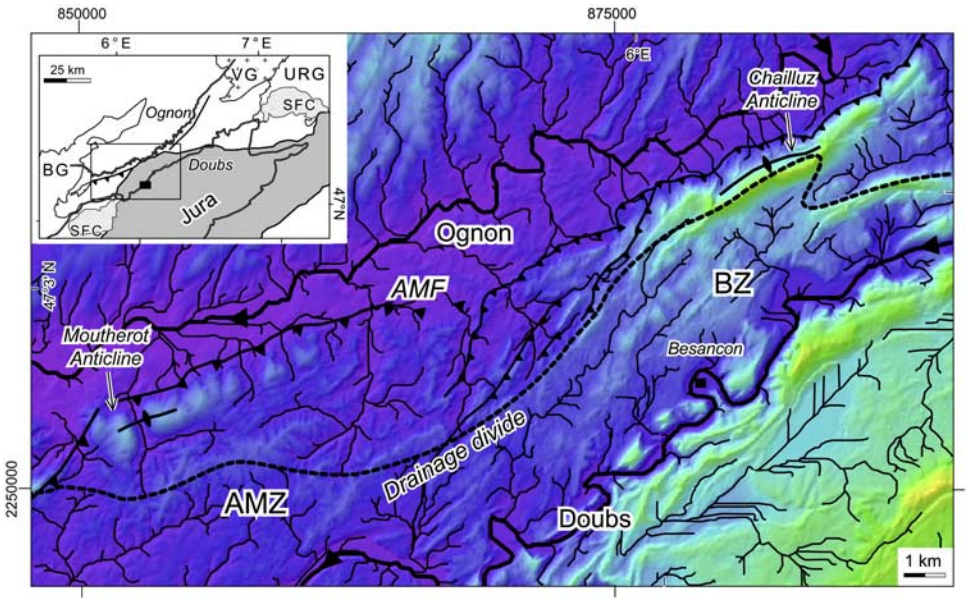

Figure 15. Synthetic drainage pattern calculated with ArcGIS software and drainage divide (dashed line) superimposed on a shaded digital elevation model (horizontal resolution 50 m). The inset in the upper left shows the regional drainage pattern and the distribution of the Sundgau and Forêt de Chaux gravels (SFC). The area is characterized by a ENE–WSW striking drainage divide between the drainage areas of the Ognon and Doubs rivers, which both flow toward the SW into the Bresse Graben (BG see inset) and by N–S trending tributary streams. Note the trend of the drainage divide that follows the boundary of the thin-skinned Besançon Zone, as well as the difference in drainage pattern of tributary streams, which reveal a consequent pattern around the thin-skinned Chailluz Anticline but which are antecedent with respect to the thick-skinned Moutherot Anticline. AMF, Avant-Monts Fault; AMZ, Avant-Monts Zone; BG, Bresse Graben; BZ, Besançon Zone; SFC, Sundgau and Forêt de Chaux gravels; URG, Upper Rhine Graben; VG, Vosges Mountains.

provenance and deposited the Sundgau and Fôret de Chaux gravels (SFC, see inset in Figure 15) in the area south of the Chailluz anticline during the middle Pliocene (4.2 to 2.9 Ma) [*Petit et al.*, 1996; *Giamboni et al.*, 2004; *Madritsch*, 2008]. Since the thin-skinned Chailluz anticline controls the location of this drainage divide it indicates a minimum age of 4.2 Ma for structural uplift related this structure. The consequent pattern of tributary streams around the fold structure implies that the rock uplift associated with folding was either too rapid for the streams to maintain their course over the anticline [*Burbank et al.*, 1996], or alternatively, the fold structure evolved prior to the tributary pattern. We favor the latter interpretation, which is constrained by the observation that no significant wind gaps can be observed along the fold crest. Moreover, during the erosion of the Sundgau and Forêt de Chaux gravels caused by post-2.9 Ma relative rock uplift along the Rhine-Bresse Transfer Zone (see distribution of SFC in the inset of Figure 15) no Alpine derived sediment was apparently shed northward beyond the Chailluz anticline into the Ognon valley [*Campy*, 1984; *Madritsch*, 2008].

[60] In contrast, the topographic barrier formed by the thick-skinned Moutherot anticline suggests that the formation of this structure postdates the late Pliocene drainage divide. The tributary stream system presently observed is older, as is evident from the antecedent pattern of streams that cut through the topographic barrier. This yields that thick-skinned deformation is characterized by low rates of associated rock uplift and onset during a late stage of the deformation history after the formation of the outermost thin-skinned anticline of Chailluz (post-4.2 Ma).

[61] Nevertheless, subsequent deformation postdating the middle Pliocene is recorded in the area south of the Chailluz Anticline and throughout the internal parts of the Besançon Zone affected by thin-skinned deformation. This is evidenced by differential erosion of the post-2.9 Ma old deformation marker horizon provided by the Sundgau and Forêt de Chaux gravels [*Campy*, 1984; *Madritsch*, 2008]. Post-mid-Pliocene folding is inferred along the thin-skinned Clerval Anticline (Figure 14). The highly sinuous Doubs river that developed out of the Paleo-Aare braided river system since the late Pliocene, which incised into the eroded Sundgau and Forêt de Chaux gravel plane (see inset of Figure 15), reveals an antecedent course with respect to the fold structure. Plio-Pleistocene terraces composed of coarse gravels of Alpine provenance are found to the north and south of the anticline [*Contini et al.*, 1973; *Madritsch*, 2008]. This indicates that fold growth along the Clerval Anticline continued after the deposition of the Sundgau and Forêt de Chaux gravels. This interpretation is constrained by the recent detection of Sundgau and Forêt de Chaux gravel remnants on top of other anticlines located north to the

Faisceau Bisontin. Within this area folding within the internal parts of the thin-skinned fold-and-thrust belt even continued into late Pleistocene times, as is evident from the differential offsets of paleomeanders recently dated by optical stimulated luminescence [*Madritsch*, 2008]. These observations are in contrast to the northern Jura front farther to the east, where post-2.9. Ma folding of the Sundgau gravel base only occurs in an area located north of the front of the thin-skinned Jura fold-and-thrust belt [*Giamboni et al.*, 2004; *Ustaszewski and Schmid*, 2007].

4. Discussion

4.1. Spatial and Temporal Interactions of Thin and Thick-Skinned Tectonics

[62] The data presented provide evidence for two contrasting styles of Neogene to recent contraction along the northwestern Jura front:

[63] 1. Thin-skinned deformation of the Jura fold-and-thrust belt that also dominates the Besançon Zone is characterized by a gently dipping, shallow décollement, penetrated by the borehole of Chailluz (Figures 6 and 8b). Paleostress directions associated with thin-skinned tectonics strike N–S to E–W and reveal a consistently fanning pattern, also detected during previous studies [*Laubscher*, 1972; *Homberg et al.*, 1999; *Ustaszewski and Schmid*, 2006].

[64] 2. Thick-skinned deformation, involving both Mesozoic cover and Paleozoic basement, takes place under more or less consistently NW–SE directions of maximum horizontal stress within the area of investigation. This deformation is associated with compressional to transpressional reactivation of preexisting normal faults of Paleogene to Paleozoic age, which also resembles observations from neighboring areas [*Giamboni et al.*, 2004; *Rotstein and Schaming*, 2004; *Ustaszewski and Schmid*, 2007].

[65] The complex structural setting at the northwestern Jura front is schematically illustrated in Figure 16 and results from spatial interferences between the two different styles of deformation. The data clearly indicate that both thin- and thick-skinned shortening postdate Paleogene extension that was associated with the formation of the European Cenozoic Rift System, as is witnessed by the reactivation of mesoscale to macroscale Paleogene normal faults. Hence, both styles of deformation are related to contraction that affected the northern Alpine foreland from the Miocene onward, as a consequence of ongoing Alpine collision [*Bergerat*, 1987; *Dèzes et al.*, 2004]. Earlier thick-skinned shortening in the area related to the late Eocene "Pyrenean" compression, as documented for more external parts of the Alpine foreland [*Lacombe and Obert*, 2000], cannot be entirely excluded. Such earlier deformation would, however, be of minor importance and completely overprinted by later tectonic events, primarily by the Eo-

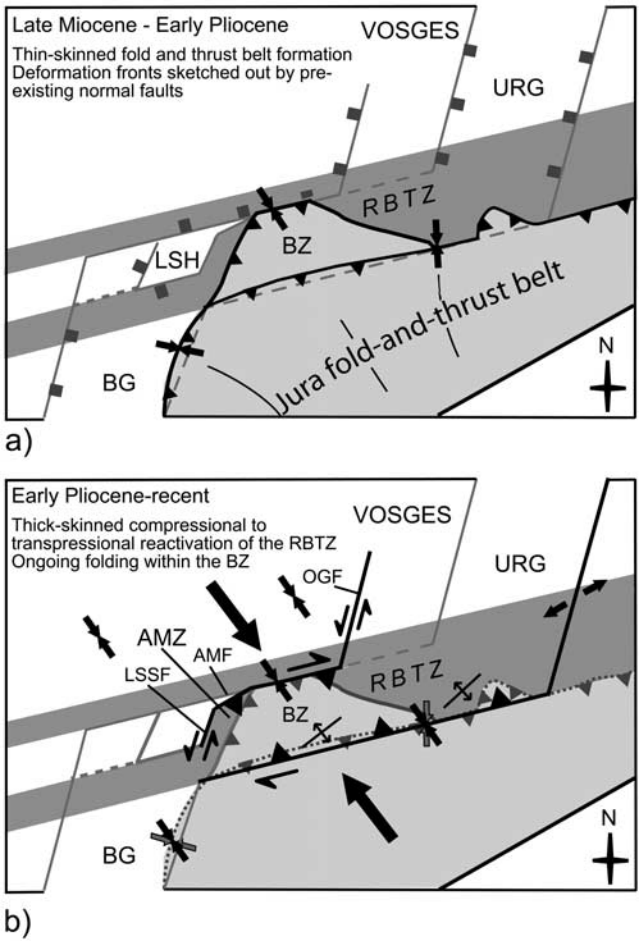

Figure 16. Sketch illustrating Neogene to present interactions between thin- and thick-skinned tectonics at the northwestern front of the Jura Mountains. (a) Late Miocene to early Pliocene development of the thin-skinned Jura fold-and-thrust belt, involving the formation of the mildly detached Besançon Zone that propagated onto the Rhine-Bresse Transfer Zone and the underlying Late Paleozoic Burgundy Trough. The thin-skinned deformation front is characterized by fanning stress trajectories and sketched out by precollisional structures. (b) Thick-skinned tectonics, best documented along the Avant-Monts Fault (AMF), and interpreted in terms of a partial compressive to dextrally transpressive reactivation of the RBTZ. Basement rooted inversion tectonics and further growth of older thin-skinned structures interfered in the Besançon Zone were deformation continued into Pleistocene times. Note that in contrast to our working area, the area of the eastern Upper Rhine Graben appears to be rather dominated by a present-day regime of transtension to strike-slip deformation [*Kastrup et al.*, 2004]. Thick black lines mark tectonically active structures. Small arrows mark paleostress trajectories as observed in this study. Large arrows mark the presumed Neogene to recent orientation of maximum principal stress (see text for further discussion). AMF, Avant-Monts Fault; AMZ, Avant-Monts Zone; BG, Bresse Graben; BZ, Besançon Zone; LSH, La Serre Horst; LSSF, La Serre Southern Fault; OGF, Ognon Fault; RBTZ, Rhine-Bresse Transfer Zone; URG, Upper Rhine Graben.

Oligocene extensional reactivation of Late Paleozoic basement structures [*Madritsch*, 2008].

[66] The propagation of the Jura fold-and-thrust belt appears to be controlled by preexisting structures, as is its northernmost front in the foreland (Figure 16a). The deformation front of the substantially detached part of the Jura fold-and-thrust belt, as defined by the Lomont, Bisontin, and Quingey faiceaux, coincides with the southern rim of the Paleogene Rhine-Bresse Transfer Zone that is inherited from the Late Paleozoic Burgundy Trough (Figures 2 and 16). The Faisceau du Lomont in the eastern part of the study area does not form a clearly defined external front of thin-skinned deformation, and this resembles the situation found along the Jura front farther to the east [*Laubscher*, 1983]. This is, for example, documented by the Clerval Anticline that is located north of the Faisceau du Lomont (Figures 8a and 14), which we interpret as representing a thin-skinned structure whose location is controlled by a preexisting normal fault. A thin-skinned style of deformation cannot be excluded for the Montbéliard Anticline neither, a structure located within the northeastward adjacent Montbéliard Plateau (Figure 3; compare *Laubscher* [1983]). However, to the east of the Montbéliard area, *Giamboni et al.* [2004] and *Ustaszewski and Schmid* [2007] provided evidence from seismic reflection data that suggests a predominance of thick-skinned tectonics in front of the eastern prolongation of the Faisceau du Lomont.

[67] The northward propagation of the only mildly displaced part of the thin-skinned Jura fold-and-thrust belt, the Besançon Zone, beyond the Faisceau du Lomont and the Faisceau Bisontin in the central part of the study area was also largely controlled by the preexisting Paleogene and Paleozoic fault pattern of the Rhine-Bresse Transfer Zone onto which the thrust sheet encroached, probably during a latest stage of thin-skinned deformation (Figure 16a). The NNE–SSW striking western boundary of the Besançon Zone coincides with a major Paleogene age normal fault that can be traced from the eastern border fault of the Bresse Graben in the south all the way into the Vesoul Plateau to the north (Figures 3 and 5). It separates the Besançon Zone from the preexisting structural high, namely, the Late Paleozoic La Serre Horst Structure that was reactivated during Eo-Oligocene extension, and it also partly includes the Avant-Monts Zone (Figures 2 and 14) [*Madritsch*, 2008]. The normal fault is inferred to have acted as a lateral ramp, inducing sinistrally transpressive deformation of the detached cover during its northward propagation. This is expressed by NNE–SSW striking folds and thrust faults mapped west of the city of Besançon, which are markedly oblique to the overall NW–SE orientation of shortening, and by a tectonic regime of transpression such as indicated by the paleostress analysis (Figures 3, 5, and 11). Possibly, the formation of this lateral ramp was related to early stage thick-skinned tectonics that interacted with the thin-skinned thrust sheet; a similar process has been described from the fold-and-thrust belt of northwestern Taiwan [*Lacombe et al.*, 2003].

[68] The existence of a lateral ramp inducing sinistrally transpressive deformation of the detached cover was also invoked for the Ferrette Jura, located east of our study area, which propagated onto the southernmost Upper Rhine Graben (FJ in Figure 1) [*Ustaszewski and Schmid*, 2006]. There, the propagation of the thin-skinned thrust sheet along a lateral ramp caused transpression and a significant gradient of shortening, the largest amounts of shortening being located close to the ramp. An analogous process is also inferred for the Besançon Zone on the basis of map view and cross sections (Figures 3, 5, and 8). Particularly, the Chailluz Anticline at the front of the Besançon Zone shows amounts of shortening that continuously decrease from west (near the Chailluz borehole) to east (see topographical expression of the anticline in Figure 5), where the boundary drawn between thin-skinned Besançon Zone and Montbéliard Plateau, largely characterized by thick-skinned deformation, had to be drawn rather artificially in Figure 3.

[69] Occurrence and location of thick-skinned deformation (Figure 16b), as observed in the Avant-Monts Zone, are also closely related to the presence of preexisting faults. As is evident from the seismic data set from this area (Figures 7 and 8c) the western segment of the Avant-Monts Faults formed by inversion of a preexisting Paleogene fault related to graben formation. Since the western prolongation of the Avant-Monts Fault abuts the La Serre Southern Fault that forms the southeastern boundary of the La Serre Massif (Figures 3 and 5) and represents a horst structure, inversion of Paleozoic structures, or combined Paleozoic and Paleogene structures, is likely. Compressive to dextrally transpressive shortening, as observed along the Avant-Monts Fault, is transferred toward the west along the La Serre Southern Fault, as can be implied by the results of the paleostress analysis that yields transpression in that area. In the eastern part of the study area the Avant-Monts Fault connects with the NNE–SSW striking Ognon Normal Fault (Figures 1, 3, 8a, and 16b). Similar to the La Serre Southern Fault it represents a major Paleogene normal fault that reactivated a Paleozoic fault traceable into the basement of the Vosges Mountains [*Ruhland*, 1959]. A mild transpressive inversion is inferred along this fault from geomorphic observations [*Theobald et al.*, 1977; *Campy*, 1984; *Madritsch*, 2008].

[70] Thick-skinned deformation is interpreted to result in the partial inversion of the intracontinental Rhine Bresse Transfer Zone and the underlying Late Paleozoic Burgundy Trough due to a change from sinistral transtension, active in the Eo-Oligocene [*Lacombe et al.*, 1993; *Madritsch*, 2008] (Figure 2), to dextral transpression from the Neogene onward [*Laubscher*, 1970; *Ustaszewski and Schmid*, 2007] (Figure 16b). However, as no surface or subsurface continuation of the Avant-Monts Fault can be traced eastward into the Rhine Graben (Figure 16b), we do not infer a throughgoing reactivation of the intracontinental Rhine-Bresse Transfer Fault Zone. Instead, we suspect that compressive to dextrally transpressive shortening during the Neogene along the western segment of the Avant-Monts Fault was not transferred all along the northern rim of Rhine-Bresse Transfer Zone toward the Rhine Graben, but was taken up and transferred by transpressive reactivation of the Ognon Normal Fault (Figures 1, 3, 8a, and 16b). Thick-skinned

partial reactivation of the Rhine-Bresse Transfer Zone spatially interferes with thin-skinned structures within the Besançon Zone where the Jura fold-and-thrust belt encroached onto the transfer zone (Figures 8b and 16b).

[71] While the coexistence of both types of deformation is well documented in the study area, the question arises as to whether these two Neogene age modes of deformation also coexisted in time [*Meyer et al.*, 1994; *Nivière and Winter*, 2000], or alternatively, if a younger thick-skinned deformation event followed older thin-skinned deformation, as was proposed by *Ustaszewski and Schmid* [2007].

[72] The brittle tectonic investigations carried out during this study lead to the conclusion that the most recent paleostress trajectories recorded in the area fairly consistently strike NW–SE and are confined by steep strike-slip faults. In the intensively deformed areas along the Bisontin, Lomont, and Quingey faisceaux these trajectories frequently overprint fanning stress trajectories related to an early stage of thin-skinned deformation (Figures 11, 16a, and 16b). The late stage persistence of the consistently NW–SE directed stress field beyond the main phase of thin-skinned folding and thrusting within the Jura fold-and-thrust belt has also been recognized in its internal parts [*Homberg et al.*, 2002]. Folding along the northern rim of the Besançon and Avant-Monts Zone persisted beyond this very latest brittle deformation stage as is evident form several faulting-folding relationships (e.g., sites 35, 36, 37, and 66). Most notably along the thick-skinned Avant-Monts Fault, a clear rotation of the youngest observed fault slip sets due to folding along the Moutherot Anticline can be observed (Figure 10), suggesting late stage activity of thick-skinned tectonics. Furthermore, geomorphic observations indicate that the thick-skinned Moutherot Anticline formed after the thin-skinned Chailluz Anticline, the latter revealing a minimum age of 4.2 Ma (Figure 15).

[73] Within in the Besançon Zone, where the different tectonic styles potentially interfere (Figures 8b and 16), crosscutting relationships can be inferred from structural data. Large-scale outcrops within the city of Besançon (Figure 17) display the main thrust fault related to the Faisceau Bisontin, a south dipping low-angle thrust fault, to be dissected by younger south facing reverse faults. These steep reverse faults are interpreted as basement-rooted former normal faults of Paleogene age that parallel the Faisceau Bisontin and form the southern rim the Rhine-Bresse Transfer Zone [*Martin and Mercier*, 1996]. Hence, they are not regarded as décollement-related back thrusts. This interpretation is largely based on the observation that the footwall of the low-angle thrust fault is characterized by steeply dipping Mesozoic strata; this is typical for extension-related flexures observed along major normal faults throughout the study area (Figures 8a and 8c) and farther to the east within the southern Upper Rhine Graben [*Ustaszewski et al.*, 2005a; *Ford et al.*, 2007]. Moreover, the occurrence of Oligocene synrift sediments along strike points to the existence of Paleogene graben structures in the area [*Glangeaud*, 1949; *Dreyfuss and Kuntz*, 1969; *Chauve et al.*, 1980]. In the light of the new subsurface data from the Avant-Monts Zone these field observations strongly suggest the interpretation that redeformation of the shallow thrust fault was caused by basement rooted thick-skinned deformation associated with inversion of preexisting basement faults.

[74] Throughout the internal parts of Besançon Zone tectonic activity related to ongoing shallow décollement along the Triassic evaporites, associated with further growth of folds that initially formed during the thin-skinned stage of deformation (early Pliocene [*Becker*, 2000; *Ustaszewski and Schmid*, 2007]), is strongly suggested given the differential erosion of the mid-Pliocene Sundgau and Forêt de Chaux gravels throughout that area [see *Campy*, 1984; *Madritsch*, 2008]. This hypothesis is constrained by the observation that active folding within parts of the Besançon Zone, occurs localized and in response to focused Pleistocene river incision [*Dreyfuss and Glangeaud*, 1950; *Madritsch*, 2008]. According to recent numerical models [*Simpson*, 2004], enhancement of deformation by this kind of surface process requires that river incision and plastic deformation by buckling occur simultaneously under regional horizontal compression.

4.2. Style of Neotectonic Deformation

[75] Data on the present-day tectonic activity within the study area are available from seismic and seismotectonic evidence, as well as from in situ borehole measurements of recent stress within the sedimentary cover. Figure 18 shows a compilation of data comprising the instrumentally recorded earthquakes with M_L magnitude larger than 3, extracted from the databases of the Réseau National de Surveillence Sismique (2007, http://renass.u-strasbg.fr/) and the Swiss Seismological Survey (Swiss Seismological Service ETHZ, Regional moment tensor catalogue, 2007, available at http://www.seismo.ethz.ch/mt/). Published focal mechanisms were compiled from various sources [*Dorel et al.*, 1983; *Bonjer et al.*, 1984; *Pavoni*, 1987; *Nicolas et al.*, 1990; *Plenefisch and Bonjer*, 1997; *Lopes Cardozo and Granet*, 2003; *Kastrup et al.*, 2004; *Baer et al.*, 2005, 2007; Swiss Seismological Service ETHZ, Regional moment tensor catalogue, 2007, available at http://www.seismo.ethz.ch/mt/]. Orientations of maximum horizontal stress $\sigma 1$ were obtained from the 2005 world stress map release [*Reinecker et al.*, 2005] and from *Becker and Werner* [1995], mostly derived from in situ borehole measurements carried out within the Mesozoic cover using the borehole slotter and doorstopper method that are discussed in detail by *Becker* [2000].

[76] Seismicity in the northern Alpine foreland is low to moderate. The Rhine-Bresse Transfer Zone shows a significantly lower activity in comparison to the Rhine Graben area [*Baer et al.*, 2007], leading to a rather poorly defined present-day stress field [*Kastrup et al.*, 2004]. The direction of $\sigma 1$ is mostly within a western or northern quadrant and hence most probably approximately strikes NW–SE. The analysis of focal depths of earthquakes clearly shows that ongoing deformation also involves the crystalline basement, all the way down to the Moho [*Deichmann et al.*, 2000]. Throughout the central Jura fold-and-thrust belt and the Rhine-Bresse Transfer Zone, earthquakes are mostly found

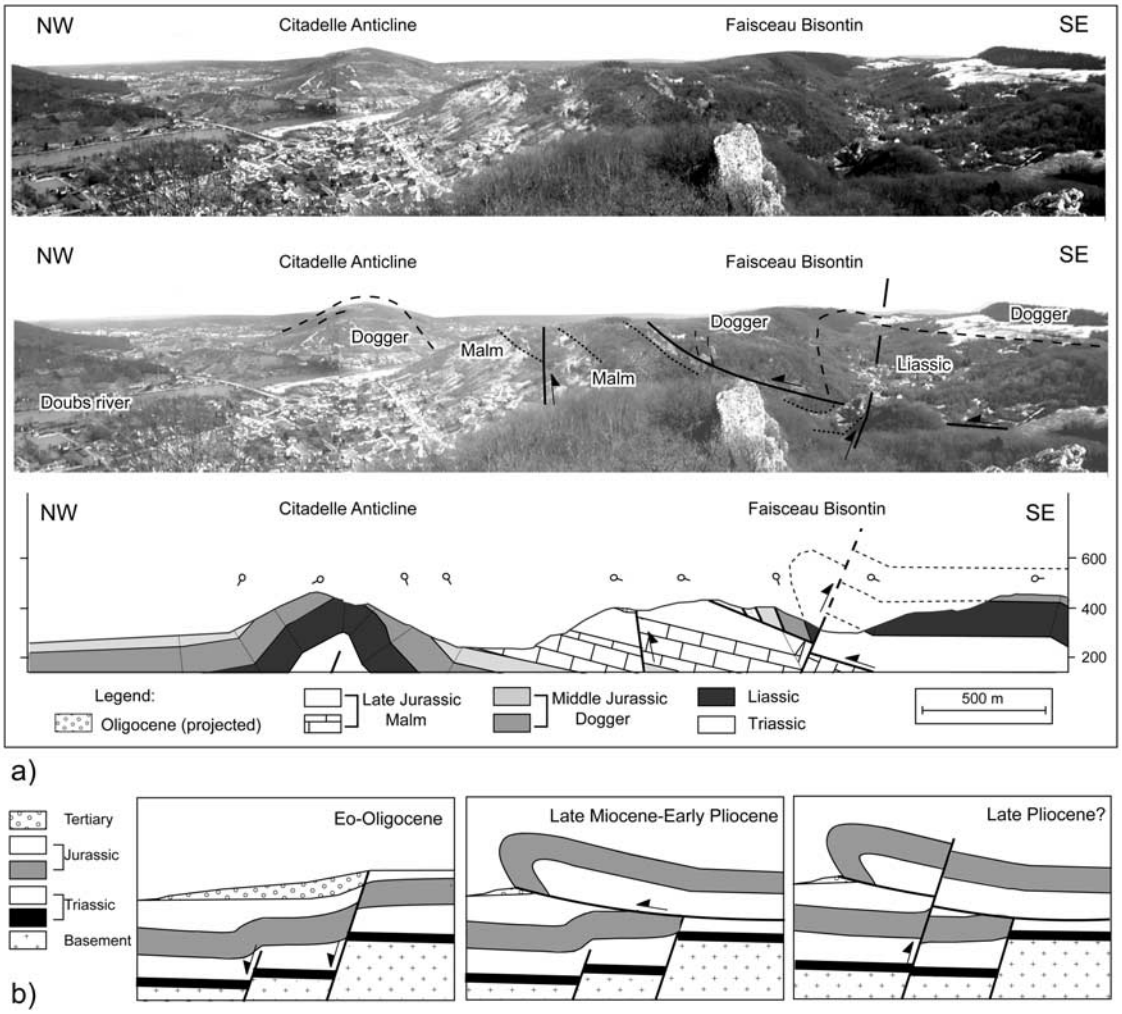

Figure 17. Section across the Faisceau Bisontin near the town of Besançon. (a) Panorama and cross section across the Faisceau Bisontin near the town of Besançon (see Figure 5 for location). Large-scale outcrops provide field evidence for an offset of the northwest facing low-angle thrust fault associated with the Faisceau Bisontin by thick-skinned steep reverse faults. (b) Sketch showing the interpretation of the evolution along this profile. Normal faults, formed during the Eo-Oligocene evolution of the Rhine-Bresse Transfer Zone, predetermine the location of the later formed steep reverse faults. Such normal faulting well explains flexuring of the Mesozoic strata in the hanging wall of the normal fault and deposition of synrift sediments nearby. During an intermediate stage the main phase of thin-skinned Jura folding the thrust fault associated with the Faisceau Bisontin was localized along the preexisting Paleogene flexure. In a third stage (late Pliocene to recent?) the normal fault was inverted, which led to the dissection of the low-angle thrust fault and top-to-the-SE superposition of its footwall over its hanging wall as observed at the outcrop.

far below the supposed thin-skinned décollement horizon, although there are also apparently shallow events, such as for example recorded around the city of Neuchâtel [*Baer et al.*, 2007]. Focal mechanisms of deep earthquakes underneath the Jura fold-and-thrust belt mostly feature strike-slip regimes. In contrast to the neighboring Rhine Graben area, which is characterized by strike-slip or transtension [*Kastrup et al.*, 2004], the deep earthquakes observed within the Rhine-Bresse Transfer Zone also reveal pure to oblique thrust faulting mechanisms [*Lopes Cardozo and Granet*, 2003; *Baer et al.*, 2005]. The surface projection of the earthquake of Besançon [*Baer et al.*, 2005] (23 February 2004; Ml 4.8; depth 15 km; marked by white square in Figure 18) that features a focal mechanism indicating oblique thrusting has been interpreted to coincide with the trace of the Avant-Monts Fault (see inset of Figure 18, modified from *Conroux et al.* [2004]). Notably, this accounts only for the fault plane solution based on first motion polarities but not the one based on full-waveform moment tensor inversion (for details, see *Baer et al.* [2005]).

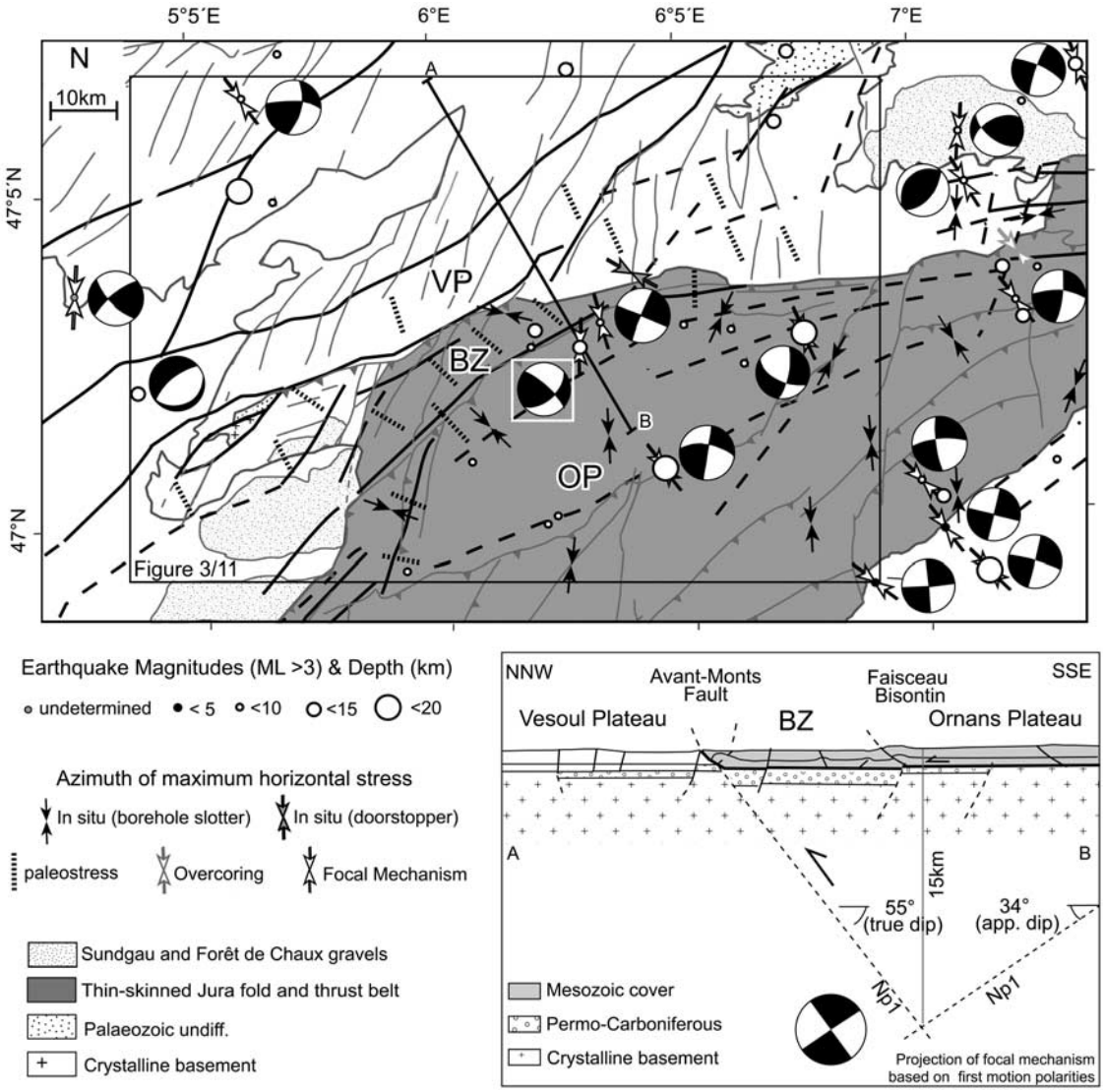

Figure 18. Neotectonic activity within the working area, as documented by focal mechanisms and in situ stress measurements from borehole slotter and doorstopper tests [*Becker and Werner*, 1995; *Becker*, 2000]. Further orientations of maximum horizontal stress are taken from the 2005 World Stress Map release [*Reinecker et al.*, 2005]. Earthquake epicenter locations and depths are taken from the databases of the Réseau National de Surveillence Sismique (2007, http://renass.u-strasbg.fr/) and the Swiss Seismological Survey (Swiss Seismological Service ETHZ, Regional moment tensor catalogue, 2007, available at http://www.seismo.ethz.ch/mt/). The focal mechanisms are compiled from various sources (see text). Stippled lines indicate the maximum horizontal shortening directions obtained from paleostress analysis during this study (compare Figure 11). Thick black lines indicate basement-rooted faults related to Late Paleozoic and Eo-Oligocene extension or transtension (modified from *Debrand-Passard and Courbouleix* [1984], *Philippe et al.* [1996], and *Ustaszewski et al.* [2005b]). Note the extent of the thin-skinned Jura fold-and-thrust belt, which also includes the newly defined Besançon Zone and the Pliocene Sundgau and Forêt de Chaux gravels that are eroded in the latter area (compare Figure 3 and 15). BZ, Besançon Zone; OP, Ornans Plateau; VP, Vesoul Plateau. The inset in the bottom right shows a simplified cross section, modified from *Conroux et al.* [2004], and illustrates the surface projection of the focal mechanism of the earthquake of Besançon (23 February 2004; Ml 4.8; depth 15 km [*Baer et al.*, 2005] marked by white square) that coincides with the trace of the Avant-Monts Fault.

[77] This evidence strongly supports the suggestion that currently active thick-skinned tectonics involves transpressional to compressional reactivation of structures related to the Paleogene Rhine-Bresse Transfer Zone and the Paleozoic Burgundy Trough System (Figure 18). Similar observations suggest basement inversion in the area along the southern boundary of the Jura fold-and-thrust belt adjacent to the Molasse basin that have been interpreted as being caused by the accretion of new basement nappes during ongoing tectonic underplating in northern Alpine foreland [*Pfiffner et al.*, 1997; *Mosar*, 1999; *Lacombe and Mouthereau*, 2002; *Ustaszewski and Schmid*, 2007].

[78] While there is ample evidence for ongoing thick-skinned tectonic activity, the question as to whether thin-skinned tectonics is still active today [*Nivière and Winter*, 2000; *Müller et al.*, 2002], or alternatively, if it ceased by early Pliocene times [*Ustaszewski and Schmid*, 2007], is more difficult to answer. On the basis of in situ stress measurement data, partly shown in Figure 18, *Becker* [2000] concluded that thin-skinned deformation did cease, on the basis of a series of arguments. He pointed out that recent stress provinces do not coincide with the tectonic zonation of the Jura Mountains and that the orientation of recent stress axes is similar in areas affected by thin-skinned deformation and areas in the foreland not affected by this style of deformation. *Becker* [2000] raised further arguments against ongoing thin-skinned tectonics such as the deviation between paleostresses and recent stresses and the parallelism of the directions of the maximum horizontal stresses derived from surface in situ stress measurements and those obtained from focal mechanisms within the basement, arguing against persisting decoupling between basement and cover.

[79] While the arguments discussed above clearly apply for the southwestern and northern part of the thrust belt, the situation is not as clear in our area of investigation, particularly within the Besançon Zone (Figure 18). As mentioned by *Becker* [2000], this is about the only area within the entire Jura fold-and-thrust belt where stress provinces defined by in situ stress measurements correlate well with the tectonic units. Unfortunately, there are not enough in situ stress data available for testing if the orientation of the present-day direction of $\sigma 1$ changes north of the Besançon Zone, i.e., outside the area affected by thin-skinned deformation. However, from the results of our paleostress analysis (compare Figure 11), one would actually expect them to be parallel in that area. Within the Besançon Zone and along the faisceaux the recent orientation of $\sigma 1$ obtained by in situ measurements almost perfectly fits the shortening directions obtained by this study (Figure 11) and they show a deviation from the $\sigma 1$ orientation obtained from nearby focal mechanisms by almost 60° in some cases. This implies that the stress field within the sedimentary cover stayed the same throughout this area from at least early Pliocene times to the present-day. Moreover, further growth of folds that initially formed during the thin-skinned stage of deformation indicates that there still is decoupling between sedimentary cover and crystalline basement. Such decoupling is likely to be rooted within the basement by fault reactivation nearby (Figure 17). Shallow thrusting probably occurs simultaneously with deep-seated thick-skinned inversion that affects the underlying basement nearby and is therefore not thin-skinned in a strict sense and according to original definition by *Chapple* [1978]. On the other hand, and in the light of insufficient knowledge about the exact geometry of the subsurface in the area, recent tectonic activity related to ongoing décollement of the Jura fold-and-thrust belt throughout the Besançon Zone cannot be excluded.

5. Conclusions

[80] This investigation leads to a new structural subdivision of the northwestern front of the Jura fold-and-thrust belt. The area located in front of the substantially detached parts of the Jura fold-and-thrust belt is divided into two parts characterized by different styles of deformation: (1) the Besançon Zone that represents the northwestern most and only mildly detached segment of the thin-skinned Jura fold-and-thrust belt that encroached onto the Rhine-Bresse Transfer Zone, and (2) the Avant-Monts Zone proper where seismic reflection data document thick-skinned shortening associated with the reactivation of preexisting normal faults of the Rhine-Bresse Transfer Zone.

[81] Paleostress analysis yields fanning north over NW to west directed orientations of maximum principal stress ($\sigma 1$) during thin-skinned deformation associated with strike-slip, transpressional, and reverse faulting. By contrast, the stable foreland and those areas affected by thick-skinned deformation are characterized by more or less constantly NW–SE directed orientation of $\sigma 1$, predominantly achieved by strike-slip faulting within the Mesozoic cover.

[82] Kinematic and geomorphic observations allow establishing a relative chronology of the different deformation styles. Thick-skinned tectonics initiated during or slightly after the latest stages of the main phase of thin-skinned Jura folding and thrusting, at the earliest at around 4.2 Ma, i.e., during the early Pliocene.

[83] Within the Besançon Zone, where the thin-skinned fold-and-thrust belt encroached onto the Rhine-Bresse Transfer Zone, deformation continued after the late Pliocene (post-2.9 Ma), as is evident from the erosion of the Sundgau and Forêt de Chaux gravels throughout that area. There is abundant structural evidence for presently ongoing thick-skinned shortening, as is confirmed by present-day seismicity. Ongoing growth of folds within the Besançon Zone that formed during an earlier thin-skinned stage of deformation appears to be positively coupled to erosion and is thus probably related to deformation along the evaporite décollement horizon. Although this deformation is likely to be rooted within the basement by fault reactivation nearby, ongoing thin-skinned deformation cannot be excluded. Hence, at the northwestern Jura front deep-seated seismogenic thick-skinned tectonics and, presumably largely aseismic, shallow décollement tectonics may interact in space and time from early Pliocene times (4.2 Ma) to the present.

[84] The results of this study highlight the crucial role of preexisting structures on the evolution of foreland fold-and-

thrust belts, also in settings where deformation is governed by classical thin-skinned tectonics. In the case of the northwestern Jura front preorogenic extensional faults first controlled the nucleation of shallow thrust faults and folds due to the offset of the décollement horizon and extensional flexuring of the sedimentary sequence. Lateral ramps inherited preexisting horst and graben structures and controlled the propagation of thin-skinned thrust sheets beyond the front of the thrust belt. Late stage thick-skinned inversion of deep-seated preexisting normal faults occasionally led to the thick-skinned redeformation of older thin-skinned structures.

[85] **Acknowledgments.** This project was funded by ELTEM and carried out within the framework of the EUCOR URGENT project. The authors are indebted to Gaz de France for the authorization to analyze and publish seismic reflection data as well as to BRGM and Total for further subsurface data provision. We also would like to thank Patrick Rolin, Kamil Ustaszewski, Pierre Dèzes, and the entire past and present Basel EUCOR-URGENT team for helpful discussions. We particularly thank the initiator of this project, Peter Ziegler, for his comments on early versions of the manuscript. Detailed and constructive reviews by Olivier Lacombe and Adrian Pfiffner significantly improved an earlier version of the manuscript.

References

Affolter, T., and J.-P. Gratier (2004), Map view retrodeformation of an arcuate fold-and-thrust belt: The Jura case, *J. Geophys. Res.*, *109*, B03404, doi:10.1029/2002JB002270.

Alvarez, W. (1999), Drainage on evolving fold-thrust belts: A study of transverse canyons in the Apennines, *Basin Res.*, *11*, 267–284, doi:10.1046/j.1365-2117.1999.00100.x.

Anderson, E. M. (1942), *The Dynamics of Faulting and Dyke Formation With Applications to Britain*, 206 pp., Oliver and Boyd, Edinburgh, U.K.

Angelier, J. (1989), From orientation to magnitudes in paleostress determinations using fault slip data, *J. Struct. Geol.*, *11*, 37–50, doi:10.1016/0191-8141(89)90034-5.

Angelier, J. (1990), Inversion of field data in fault tectonics to obtain the regional stress. III. A new rapid direct inversion method by analytical means, *Geophys. J. Int.*, *103*, 363–376, doi:10.1111/j.1365-246X.1990.tb01777.x.

Angelier, J., and P. Mechler (1977), Sur une méthode graphique de recherche des contraintes principales également utilisable en tectonique et en seismologie: La méthode des dièdres droits, *Bull. Soc. Geol. Fr.*, *19*, 1309–1318.

Aubert, D. (1945), Le Jura e la tectonique d'écoulement, *Mem. Soc. Vaud. Sci. Nat.*, *8*, 217–236.

Baer, M., N. Deichmann, J. Braunmiller, S. Husen, D. Fäh, D. Giardini, P. Kästli, U. Kradolfer, and S. Wiemer (2005), Earthquakes in Switzerland and surrounding regions during 2004, *Eclogae Geol. Helv.*, *98*, 407–418, doi:10.1007/s00015-005-1168-3.

Baer, M., N. Deichmann, J. Braunmiller, J. Clinton, S. Husen, D. Fäh, D. Giardini, P. Kästli, U. Kradolfer, and S. Wiemer (2007), Earthquakes in Switzerland and surrounding regions during 2006, *Swiss J. Geosci.*, *100*, 517–528, doi:10.1007/s00015-007-1242-0.

Becker, A. (2000), The Jura Mountains—An active foreland fold-and-thrust belt?, *Tectonophysics*, *321*, 381–406, doi:10.1016/S0040-1951(00)00089-5.

Becker, A., and D. Werner (1995), Neotectonic state of stress in the Jura mountains, *Geodin. Acta*, *8*, 99–111.

Bergerat, F. (1977), La fraturaction de l'avant-pays jurassien entre les fossés de la Saône et du Rhin. Analyse et essai d'interpretation dynamique, *Rev. Geogr. Phys. Geol. Dyn.*, *14*(2), 325–338.

Bergerat, F. (1987), Stress fields in the European Platform at the time of Africa-Eurasia collision, *Tectonics*, *6*, 99–132, doi:10.1029/TC006i002p00099.

Bergerat, F., and J. Chorowicz (1981), Etude des images Landsat de la zone tranformante Rhin-Saône (France), *Geol. Rundsch.*, *70*, 354–367, doi:10.1007/BF01764334.

Boigk, H., and H. Schönreich (1970), Die Tiefenlage der Permbasis im nördlichen Teil des Oberrheingrabens, in *Graben Problems. Proceedings of an International Rift Symposium Karlsruhe 1968, International Upper Mantle Project*, edited by J. H. Illies and S. Mueller, pp. 45–55, E. Schweitzerbart'sche, Stuttgart, Germany.

Bolliger, T., B. Engesser, and M. Weidmann (1993), Première découverte de mammifères pliocènes dans le Jura neuchâtelois, *Eclogae Geol. Helv.*, *86*, 1031–1068.

Bonjer, K.-P., C. Gelbke, B. Gilg, D. Rouland, D. Mayer-Rosa, and B. Massinion (1984), Seismicity and dynamics of the Upper Rhine Graben, *J. Geophys.*, *55*, 1–12.

Bonte, A. (1975), Carte géologique de la France, scale 1:50,000, feuille Quingey, XXXIII-24, Bur. de Rech. Géol. et Min., Orléans, France.

Bourgeois, O., M. Ford, C. Diraison, M. Le Carlier de Veslud, R. Gerbault, and N. Pik (2007), Separation of rifting and lithospheric folding signatures in the NW-Alpine foreland, *Int. J. Earth Sci.*, *96*, 1003–1031, doi:10.1007/s00531-007-0202-2.

Brudy, M., M. D. Zoback, K. Fuchs, F. Rumel, and J. Baumgärtner (1997), Estimation of the complete stress tensors to 8 km depth in the KTB scientific drilling holes: Implications for crustal strength, *J. Geophys. Res.*, *102*, 18,453–18,475, doi:10.1029/96JB02942.

Bull, W. B. (1990), Stream-terrace genesis: Implications for soil development, *Geomorphology*, *3*, 351–367, doi:10.1016/0169-555X(90)90011-E.

Burbank, D., A. Meigs, and N. Brozovic (1996), Interactions of growing folds and coeval depositional systems, *Basin Res.*, *8*, 199–223, doi:10.1046/j.1365-2117.1996.00181.x.

Burkhard, M. (1990), Aspects of the large-scale Miocene deformation in the most external part of the Swiss Alps (Subalpine Molasse to Jura fold belt), *Eclogae Geol. Helv.*, *83*, 559–583.

Burkhard, M., and A. Sommaruga (1998), Evolution of the western Swiss Molasse basin: Structural relations with the Alps and the Jura belt, in *Cenozoic Foreland Basins of Western Europe*, edited by A. Mascle et al., *Geol. Soc. Spec. Publ.*, *134*, 279–298.

Buxtorf, A. (1907), Geologische Beschreibung des Weissenstein Tunnels und seiner Umgebung, in *Beiträge der Geologischen Karte der Schweiz*, Schweiz. Geol. Kom., Bern, Germany.

Calabrò, R. A., S. Corrado, D. Di Bucci, P. Robustini, and M. Tornaghi (2003), Thin-skinned vs. thick- skinned tectonics in the Matese Massif, central-southern Apennines, *Tectonophysics*, *337*, 269–297.

Campy, M. (1984), Signification dynamique et climatique des formations et terrasses fluviatiles dans un environnement de moyenne montagne, *Bull. Assoc. Fr. Etude Quat.*, *1*, 87–92.

Chapple, W. M. (1978), Mechanics of thin-skinned fold-and-thrust belts, *Geol. Soc. Am. Bull.*, *89*, 1189–1198, doi:10.1130/0016-7606(1978)89<1189:MOTFB>2.0.CO;2.

Chauve, P., R. Enay, P. Fluck, and C. Sittler (1980), L'Est de la France (Vosges, Fossé Rhénan, Bresse, Jura), *Ann. Sci. Univ. Besancon*, *4*, 3–80.

Chauve, P., M. Campy, C. Pernin, and N. Morre-Biot (1983), Carte géologique de la France, scale 1:50,000, feuille Pesmes, XXXII-23, Bur. de Rech. Géol. et Min., Orléans, France.

Conroux, Y., O. Fabbri, T. Lebourg, V. Bichet, and C. Petit (2004), Geological and geophysical investigations along a late Variscan fault exposed near the 23/02/2004 Besancon earthquake epicentral area, Réunion des Sci. de la Terre–Geol. Verein., Strasbourg, France.

Contini, D., G. Kuntz, B. Angély, J. L. Laffly, Y. Kerrien, J. Landry, and N. Théobald (1973), Carte géologique de la France, scale 1:50,000, feuille Montbéliard, XXXV-22, BRGM.

Coromina, G., and O. Fabbri (2004), Late Palaeozoic NE–SW ductile-brittle extension in the La Serre horst, eastern France, *C. R. Geosci.*, *336*, 75–84, doi:10.1016/j.crte.2003.09.019.

Costa, E., and B. C. Vendeville (2002), Experimental insights on the geometry and kinematics of fold-and- thrust belts above weak, viscous evaporitic décollement, *J. Struct. Geol.*, *24*, 1729–1739, doi:10.1016/S0191-8141(01)00169-9.

Coward, M. P. (1983), Thrust tectonics, thin skinned or thick skinned, and the continuation of thrusts to deep in the crust, *J. Struct. Geol.*, *5*, 113–123, doi:10.1016/0191-8141(83)90037-8.

Davis, D., J. Suppe, and F. A. Dahlen (1983), Mechanics of fold-and-thrust-belts and accretionary wedges, *J. Struct. Geol.*, *88*, 1153–1172.

Debrand-Passard, S., and S. Courbouleix (1984), *Synthèse Géologique du Sud-Est de la France*, vol. 2, *Mem. Bur. Rech. Geol. Min.*, *126*, 614 pp.

Deichmann, N., D. Ballarin Dolfin, and U. Kastrup (2000), *Seismizität der Nord- und Zentralschweiz*, 94 pp., Natl. Genossensch. für die Lagerung radioakt. Abfälle, Wettingen, Germany.

Dèzes, P., S. M. Schmid, and P. A. Ziegler (2004), Evolution of the European Cenozoic Rift System: Interaction of the Alpine and Pyrenean orogens with their foreland lithosphere, *Tectonophysics*, *389*, 1–33, doi:10.1016/j.tecto.2004.06.011.

Diebold, P., and T. Noack (1997), Late Palaeozoic troughs and Tertiary structures in the eastern folded Jura, in *Deep Structure of the Swiss Alps: Results of NRP 20*, edited by O. A. Pfiffner et al., pp. 59–63, Birkhäuser, Basel, Switzerland.

Dorel, J., F. Frechet, J. Ganepain-Beyneix, H. Haessler, M. Lachaize, R. Madariaga, T. Modiano, G. Pascal, G. Perrier, H. Philip, D. Rouland, and G. G. Wittlinger (1983), Focal mechanism in metropolitan France and the lesser Antilles, *Ann. Geophys.*, *1*, 299–306.

Dreyfuss, M., and L. Glangeaud (1950), La valée de Doubs et l'évolution morphotectonique de la région bisontine, *Ann. Sci. Univ. Besançon*, *5*, 2.

Dreyfuss, M., and G. Kuntz (1969), Carte géologique de la France, scale 1:50,000, feuille Besancon, XXXII-23, Bur. de Rech. Géol. et Min., Orléans, France.

Dreyfuss, M., and G. Kuntz (1970), Carte géologique de la France, scale 1:50,000, feuille Gy, XXXIII-22, Bur. de Rech. Géol. et Min., Orléans, France.

Dreyfuss, M., and N. Théobald (1972), Carte géologique de la France, scale 1:50,000, feuille Baume-les-Dames, XXXIV-22, Bur. de Rech. Géol. et Min., Orléans, France.

Ford, M., C. Le Carlier de Veslud, and O. Bourgeois (2007), Kinematic and geometric analysis of fault related folds in a rift setting: The Dannemarie basin, Upper Rhine Graben, France, *J. Struct. Geol.*, *29*, 1811–1830, doi:10.1016/j.jsg.2007.08.001.

Giamboni, M., K. Ustaszewski, S. M. Schmid, M. E. Schumacher, and A. Wetzel (2004), Plio-Pleistocene transpressional reactivation of Paleozoic and Paleogene structures in the Rhine-Bresse Transform Zone (northern Switzerland and eastern France), *Int. J. Earth Sci.*, *93*, 207–223, doi:10.1007/s00531-003-0375-2.

Glangeaud, L. (1949), Les caractères structuraux du Jura, *Bull. Soc. Geol. Fr.*, *19*, 669–688.

Guellec, S., J. L. Mugnier, M. Tardy, and F. Roure (1990), Neogene evolution of the western Alpine foreland in the light of ECORS data and balanced cross-sections, in *Deep Structure of the Alps*, *Vol. Spec. Soc. Geol. Ital.*, vol. 1, edited by F. Roure, P. Heitzmann, and R. Polino, pp. 165–184, Soc. Geol. Ital., Rome.

Guerler, B., L. Hauber, and M. Schwander (1987), Die Geologie der Umgebung von Basel mit Hinweisen über die Nutzungsmöglichkeiten der Erdwärme, *Beitr. Geol. Karte Schweiz.*, *160*, p. 33, Schweiz. Geol. Kom., Bern, Germany.

Hindle, D., and M. Burkhard (1999), Strain, displacement and rotation associated with the formation of curvature in fold belts; the example of the Jura arc, *J. Struct. Geol.*, *21*, 1089–1101, doi:10.1016/S0191-8141(99)00021-8.

Homberg, C., O. Lacombe, J. Angelier, and F. Bergerat (1999), New constraints for indentation mechanisms in arcuate belts from the Jura Mountains, France, *Geology*, *27*(9), 827–830, doi:10.1130/0091-7613(1999)027<0827:NCFIMI>2.3.CO;2.

Homberg, C., F. Bergerat, Y. Philippe, O. Lacombe, and J. Angelier (2002), Structural inheritance and Cenozoic stress fields in the Jura fold-and-thrust belt (France), *Tectonophysics*, *357*, 137–158, doi:10.1016/S0040-1951(02)00366-9.

Illies, J. H. (1972), The Rhinegraben rift system—Plate tectonics and transform faulting, *Geophys. Surv.*, *1*, 27–60, doi:10.1007/BF01449550.

Illies, J. H., and G. Greiner (1978), Rhine graben and alpine system, *Geol. Soc. Am. Bull.*, *89*, 770–782, doi:10.1130/0016-7606(1978)89<770:RATAS>2.0.CO;2.

Kälin, D. (1997), Litho- und Biostratigraphie der mittel- bis obermiozänen Bois de Raube-Formation (Nordwestschweiz), *Eclogae Geol. Helv.*, *90*, 97–114.

Kastrup, U., M. L. Zoback, N. Deichmann, K. F. Evans, D. Giardini, and A. J. Michael (2004), Stress field variations in the Swiss Alps and the northern Alpine foreland derived from inversion of fault plane solutions, *J. Geophys. Res.*, *109*, B01402, doi:10.1029/2003JB002550.

Lacombe, O., and F. Mouthereau (2002), Basement-involved shortening and deep detachment tectonics in forelands of orogens: Insights from recent collision belts (Taiwan, Western Alps, Pyrenees), *Tectonics*, *21*(4), 1030, doi:10.1029/2001TC901018.

Lacombe, O., and D. Obert (2000), Héritage structural et déformation de couverture: Plissement et fracturation tertiares dans l'Ouest du Bassin de Paris, *C. R. Acad. Sci. Paris, Ser. II*, *330*, 793–797.

Lacombe, O., J. Angelier, D. Byrne, and J. Dupin (1993), Eocene-Oligocene tectonics and kinematics of the Rhine-Saone continental transform zone (eastern France), *Tectonics*, *12*, 874–888, doi:10.1029/93TC00233.

Lacombe, O., F. Mouthereau, J. Angelier, H.-T. Chu, and J.-C. Lee (2003), Frontal curvature and oblique ramp development at an oblique ramp development at an obliquely collided irregular margin: Geometry and kinematics of the NW Taiwan fold-thrust belt, *Tectonics*, *22*(3), 1025, doi:10.1029/2002TC001436.

Lacombe, O., F. Mouthereau, S. Kargar, and B. Meyer (2006), Late Cenozoic and modern stress fields in the western Fars (Iran): Implications for the tectonic and kinematic evolution of central Zagros, *Tectonics*, *25*, TC1003, doi:10.1029/2005TC001831.

Laubscher, H. (1961), Die Fernschubhypothese der Jurafaltung, *Eclogae Geol. Helv.*, *54*, 222–282.

Laubscher, H. (1970), Grundsätzliches zur Tektonik des Rheingrabens, in *Graben Problems. Proceedings of an International Rift Symposium held in Karlsruhe 1968, International Upper Mantle Project*, edited by J. H. Illies and S. Mueller, pp. 79–86, E. Schweitzerbart'sche, Stuttgart, Germany.

Laubscher, H. (1972), Some overall aspects of Jura dynamics, *Am. J. Sci.*, *272*, 293–304.

Laubscher, H. (1978), Foreland folding, *Tectonophysics*, *47*, 325–337, doi:10.1016/0040-1951(78)90037-9.

Laubscher, H. (1983), Ueberschiebungen im Jura, *Jahresber. Mitt. Oberrheinischen. Geol. Ver.*, *65*, 181–189.

Laubscher, H. (1986), The eastern Jura: Relations between thin-skinned and basement tectonics, local and regional, *Geol. Rundsch.*, *75*, 535–553, doi:10.1007/BF01820630.

Letouzey, J. (1986), Cenozoic paleo-stress pattern in the Alpine Foreland and structural interpretation in a platform basin, *Tectonophysics*, *132*, 215–231, doi:10.1016/0040-1951(86)90033-8.

Lopes Cardozo, G. G. O., and M. Granet (2003), New insight in the tectonics of the southern Rhine Graben-Jura region using local earthquake seismology, *Tectonics*, *22*(6), 1078, doi:10.1029/2002TC001442.

Madritsch, H. (2008), Structural evolution and neotectonics of the Rhine-Bresse Transfer Zone, Ph.D. thesis, Univ. of Basel, Basel.

Marrett, R., and R. W. Allmendinger (1990), Kinematic analysis of fault-slip data, *J. Struct. Geol.*, *12*, 973–986, doi:10.1016/0191-8141(90)90093-E.

Marrett, R., and D. C. P. Peacock (1999), Strain and stress, *J. Struct. Geol.*, *21*, 1061–1067.

Martin, J., and E. Mercier (1996), Héritage distensif et structuration chevauchante dans une chaîne de couverture: Apport de l'équilibrage par modélisation géométrique dans le Jura nord-occidental, *Bull. Soc. Geol. Fr.*, *167*, 101–110.

McCann, T., C. Pascal, M. J. Timmerman, P. Krzywiec, J. López-Gómez, A. Wetzel, C. M. Krawczyk, H. Rieke, and J. Lamarche (2006), Post-Variscan (end Carboniferous-Early Permian) basin evolution in western and central Europe, in *European Lithosphere Dynamics*, edited by D. G. Gee and R. A. Stephenson, *Mem. Geol. Soc. London*, *32*, 355–388.

Merritts, D. J., K. R. Vincent, and E. E. Wohl (1994), Long river profiles, tectonism and eustasy: A guide to interpreting fluvial terraces, *J. Geophys. Res.*, *99*, 14,031–14,050, doi:10.1029/94JB00857.

Meschede, M., and K. Decker (1993), Störungsflächenanalyse entlang des Nordrandes der Ostalpen—Ein methodischer Vergleich, *Z. Dtsch. Geol. Ges.*, *144*, 419–433.

Meyer, B., R. Lacassin, J. Brulhet, and B. Mouroux (1994), The Basel 1356 earthquake: Which fault produced it?, *Terra Nova*, *6*, 54–63, doi:10.1111/j.1365-3121.1994.tb00633.x.

Molinaro, M., J.-C. Leturmy, D. Guezou, D. Frizon De Lamotte, and S. A. Eshraghi (2005), The structure and kinematics of the southeastern Zagros fold-thrust belt Iran: From thin-skinned to thick-skinned tectonics, *Tectonics*, *24*, TC3007, doi:10.1029/2004TC001633.

Mosar, J. (1999), Present-day and future tectonic underplating in the western Swiss Alps: Reconciliation of basement/wrench-faulting and décollement folding of the Jura and Molasse basin in the Alpine foreland, *Earth Planet. Sci. Lett.*, *173*, 143–155, doi:10.1016/S0012-821X(99)00238-1.

Mouthereau, F., J. Tensi, N. Bellahsen, O. Lacombe, T. De Boisgrollier, and S. Kargar (2007), Tertiary sequence of deformation in a thin-skinned/thick-skinned collision belt: The Zagros Folded Belt (Fars, Iran), *Tectonics*, *26*, TC5006, doi:10.1029/2007TC002098.

Müller, W. H., H. Naef, and H. R. Graf (2002), Geologische Entwicklung der Nordschweiz, Neotektonik und Langzeitszenarien, Züricher Weinland, *Tech. Rep. 99-08*, 226 pp., Natl. Genossensch. für die Lagerung radioakt. Abfälle, Wettingen, Germany.

Nicolas, M., M. Santoire, and P. Y. Delpech (1990), Intraplate seismicity: New seimotectonic data in western Europe, *Tectonophysics*, *179*, 27–54, doi:10.1016/0040-1951(90)90354-B.

Nivière, B., and T. Winter (2000), Pleistocene northwards fold propagation of the Jura within the southern Upper Rhine Graben: Seismotectonic implications, *Global Planet. Change*, *27*, 263–288, doi:10.1016/S0921-8181(01)00070-4.

Oberlander, T. M. (1985), Origin of drainage transverse to structures in orogens, in *Tectonic Geomorphology* edited by M. Morisawa and J. T. Hack, pp. 155–182, Allen and Unwin, Boston, Mass.

Pavoni, N. (1961), Faltung durch Horizontalverschiebung, *Eclogae Geol. Helv.*, *54*, 515–534.

Pavoni, N. (1987), Zur Seismotektonik der Nordschweiz, *Eclogae Geol. Helv.*, *80*, 461–472.

Petit, J. P. (1987), Criteria for the sense of movement on fault surfaces in brittle rocks, *J. Struct. Geol.*, *9*, 597–608, doi:10.1016/0191-8141(87)90145-3.

Petit, C., M. Campy, J. Chaline, and J. Bonvalot (1996), Major palaeohydrographic changes in Alpine foreland during the Pliocene-Pleistocene, *Boreas*, *25*, 131–143.

Pfiffner, O. A. (2006), Thick-skinned and thin-skinned styles of continental contraction, in *Styles of Continental Contraction*, edited by S. Mazzoli and R. W. H. Butler, *Spec. Pap. Geol. Soc. Am.*, *414*, 153–177.

Pfiffner, O. A., and M. Burkhard (1987), Determination of paleo-stress axes orientations from fault, twin and earthquake data, *Ann. Tectonicae*, *1*, 48–57.

Pfiffner, O. A., P. Erard, and M. Stäuble (1997), Two cross sections through the Swiss Molasse Basin (lines E4–E6, W1, W7–W10), in *Deep Structure of the Swiss Alps: Results of NRP 20*, edited by O. A. Pfiffner et al., pp. 64–72, Birkhäuser, Basel, Switzerland.

Philippe, Y., B. Colletta, E. Deville, and A. Mascle (1996), The Jura fold-and-thrust belt: A kinematic model based on map-balancing, in *Peri-Tethys Memoir 2: Structure and Prospects of Alpine Basins and Forelands*, edited by P. Ziegler and F. Horvath, *Mem. Mus. Nat. Hist. Nat.*, *170*, 235–261.

Plenefisch, T., and K. Bonjer (1997), The stress field in the Rhine Graben area inferred from earthquake focal mechanisms and estimation of frictional parameters, *Tectonophysics*, *275*, 71–97, doi:10.1016/S0040-1951(97)00016-4.

Pollard, D. D., S. D. Saltzer, and A. M. Rubin (1993), Stress inversion methods: Are they based on faulty assumption?, *J. Struct. Geol.*, *15*, 1045–1054, doi:10.1016/0191-8141(93)90176-B.

Rat, P. (1976), Structures et phases de structuration dans les plateaux bourguignons et le Nord Ouest du fossé bressan (France), *Geol. Rundsch.*, *65*, 101–126, doi:10.1007/BF01808458.

Reinecker, J., O. Heidbach, M. Tingay, B. Sperner, and B. Mueller (2005), The 2005 release of the World Stress Map. (Available at http://www.world-stress-map.org)

Rocher, M., F. Chevalier, C. Petit, and M. Guiraud (2003), Tectonics of the Northern Bresse region (France) during the Alpine cycle, *Geodin. Acta*, *16*, 131–147, doi:10.1016/j.geoact.2003.05.001.

Rocher, M., M. Cushing, F. Lemeille, Y. Lozac'h, and J. Angelier (2004), Intraplate paleostresses reconstructed with calcite twinning and faulting: Improved method and application to the eastern Paris Basin (Lorraine, France), *Tectonophysics*, *387*, 1–21, doi:10.1016/j.tecto.2004.03.002.

Rotstein, Y., and M. Schaming (2004), Seismic Reflection evidence for thick-skinned tectonics in the northern Jura, *Terra Nova*, *16*, 250–256, doi:10.1111/j.1365-3121.2004.00560.x.

Ruhland, M. (1959), Une dislocation majeure du socle Vosgien dans la haute Vallée de l'Ognon, *Bull. Serv. Carte Geol. Alps Lorr.*, *12*, 61–64.

Schmid, S. M., O. A. Pfiffner, N. Froitzheim, G. Schönborn, and E. Kissling (1996), Geophysical-geological transect and tectonic evolution of the Swiss-Italian Alps, *Tectonics*, *15*, 1036–1064, doi:10.1029/96TC00433.

Schumacher, M. E. (2002), Upper Rhine Graben: Role of preexisting structures during rift evolution, *Tectonics*, *21*(1), 1006, doi:10.1029/2001TC900022.

Simpson, G. (2004), Role of river incison in enhancing deformation, *Geology*, *32*, 341–344, doi:10.1130/G20190.2.

Sissingh, W. (2001), Tectonostratigraphy of the West Alpine Foreland: Correlation of Tertiary sedimentary sequences, changes in eustatic sea-level and stress regimes, *Tectonophysics*, *333*, 361–400, doi:10.1016/S0040-1951(01)00020-8.

Smit, J. H. W., J. P. Brun, and D. Sokoutis (2003), Deformation of brittle-ductile thrust wedges in experiments and nature, *J. Geophys. Res.*, *108*(B10), 2480, doi:10.1029/2002JB002190.

Sommaruga, A. (1997), Geology of the central Jura and the Molasse Basin: New insights into an evaporite-based foreland fold and thrust belt, Ph.D. thesis, 176 pp., Schweiz. Akad. der Naturwissenschaf., Neuchatel.

Sommaruga, A., and M. Burkhard (1997), Jura Mountains, in *Deep Structure of the Swiss Alps: Results of NRP 20*, edited by O. A. Pfiffner et al., pp. 45–53, Birkhäuser, Basel, Switzerland.

Spang, J. H. (1972), Numerical method for dynamic analysis of calcite twin lamellae, *Geol. Soc. Am. Bull.*, *83*(2), 467–472, doi:10.1130/0016-7606(1972)83[467:NMFDAO]2.0.CO;2.

Sperner, B., R. Ott, and L. Ratschbacher (1993), Fault-striae analysis: A turbo pascal program package for graphical presentation and reduced stress-tensor calculation, *Comput. Geosci.*, *19*(9), 1361–1388, doi:10.1016/0098-3004(93)90035-4.

Steininger, F. F., W. A. Berggren, D. V. Kent, R. L. Bernor, S. Sen, and J. Agusti (1996), Circum-Mediterranean Neogene (Miocene and Pliocene) marine-continental chronologic correlations of European Mammal Units, in *The Evolution of Western Eurasian Neogene Mammal Faunas*, edited by R. L. Bernor, V. Fahlbusch, and H.-W. Mittmann, pp. 7–46, Columbia Univ. Press, New York.

Suppe, J. (1983), Geometry and kinematics of fault-bend folding, *Am. J. Sci.*, *283*, 684–721.

Theobald, N., H. Vogt, and O. Wittmann (1977), Néotectonique de la partie méridionale du bloc rhénan, *Bull. BRGM*, *2*(4), 121–140.

Tozer, R. S. J., R. W. H. Butler, and S. Corrado (2002), Comparing thin- and thick-skinned thrust tectonic models of the central Apennines, Italy, in *Continental Collision and the Tectono-sedimentary Evolution of Forelands*, *EUG Stephan Mueller Publ. Ser.*, vol. 1, edited by B. Bertotti, K. Schulmann, and S. A. P. L. Cloetingh, pp. 181–194, Copernicus, Katlenburg-Lindau, Germany.

Twidal, C. R. (2004), River patterns and their meaning, *Earth Sci. Rev.*, *67*(3–4), 159–219, doi:10.1016/j.earscirev.2004.03.001.

Twiss, R. J., and J. R. Unruh (1998), Analysis of fault slip inversions: Do they constrain stress or strain rate?, *J. Geophys. Res.*, *103*, 12,205–12,222, doi:10.1029/98JB00612.

Ustaszewski, K., and S. M. Schmid (2006), Control of preexisting faults on geometry and kinematics in the northernmost part of the Jura fold-and-thrust belt, *Tectonics*, *25*, TC5003, doi:10.1029/2005TC001915.

Ustaszewski, K., and S. M. Schmid (2007), Latest Pliocene to recent thick-skinned tectonics at the Upper Rhine Graben–Jura Mountains junction, *Swiss J. Geosci.*, *100*, 293–312, doi:10.1007/s00015-007-1226-0.

Ustaszewski, K., M. E. Schumacher, and S. M. Schmid (2005a), Simultaneous normal faulting and extensional flexuring during rifting: An example from the southernmost Upper Rhine Graben, *Int. J. Earth Sci.*, *94*, 680–696, doi:10.1007/s00531-004-0454-z.

Ustaszewski, K., M. E. Schumacher, S. M. Schmid, and D. Nieuwland (2005b), Fault reactivation in brittle-viscous wrench systems: Dynamically scaled analogue models and application to the Rhine-Bresse Transfer Zone, *Quat. Sci. Rev.*, *24*, 363–380, doi:10.1016/j.quascirev.2004.03.015.

Wallace, R. E. (1951), Geometry of shearing stress and relation to faulting, *J. Geol.*, *59*, 118–130.

Ziegler, P. (1986), Geodynamic model for the Paleozoic crustal consolidation of western and central Europe, *Tectonophysics*, *126*, 303–328, doi:10.1016/0040-1951(86)90236-2.

Ziegler, P. A. (1992), European Cenozoic rift system, *Tectonophysics*, *208*, 91–111, doi:10.1016/0040-1951(92)90338-7.

Ziegler, P. A., G. Bertotti, and S. A. P. L. Cloetingh (2002), Dynamic processes controlling foreland development—Role of mechanical (de)coupling of orogenic wedges and forelands, in *Continental Collision and the Tectono-sedimentary Evolution of Forelands*, *EUG Stephan Mueller Publ. Ser.*, vol. 1, edited by B. Bertotti, K. Schulmann, and S. A. P. L. Cloetingh, pp. 17–56, Copernicus, Katlenburg-Lindau, Germany.

O. Fabbri, UMR Chrono-Envrionnement, Université de Franche-Comté, Route de Gray 16, F-25030 Besançon CEDEX, France. (olivier.fabbri@univ-fcomte.fr)

H. Madritsch and S. M. Schmid, Geologisch-Paläontologisches Institut, University of Basel, Bernoullistr. 32, CH-4056 Basel, Switzerland. (herfried.madritsch@unibas.ch; stefan.schmid@unibas.ch)